1-2016

Nuclear Import of the Thyroid Hormone Receptor α1 is Mediated by Importin 7, Importin β1, and Adaptor Importin α1

Vincent R. Roggero
William & Mary, vrrogg@wm.edu

Jibo Zhang

Laura E. Parente

Yazdi Doshi

Lizabeth A. Allison
William & Mary, laalli@wm.edu

Recommended Citation

Roggero, Vincent R.; Zhang, Jibo; Parente, Laura E.; Doshi, Yazdi; and Allison, Lizabeth A., Nuclear Import of the Thyroid Hormone Receptor α1 is Mediated by Importin 7, Importin β1, and Adaptor Importin α1 (2016). *Molecular and Cellular Endocrinology*, 419(C), 185-197.
https://doi.org/10.1016/j.mce.2015.10.016

Nuclear Import of the Thyroid Hormone Receptor α1 is Mediated by Importin 7, Importin β1, and Adaptor Importin α1

Vincent R. Roggero[a], Jibo Zhang[a], Laura E. Parente[a], Yazdi Doshi[a], Rose C. Dziedzic[a], Emma L. McGregor[a], Arev D. Varjabedian[a], Sara E. Schad[a], Cornelius Bondzi[b], Lizabeth A. Allison[a*]

[a]Department of Biology, College of William and Mary, Williamsburg, Virginia, 23185, USA
[b]Department of Biological Sciences, Hampton University, Hampton, Virginia, 23668, USA

*Corresponding author. Department of Biology, College of William and Mary, 540 Landrum Dr., ISC 2117, Williamsburg, Virginia 23185, USA. Tel.: +1 757 221-2232; Fax: +1 757 221-6483; E-mail address: laalli@wm.edu (L. A. Allison)

Abstract

The thyroid hormone receptor α1 (TRα1) is a nuclear receptor for thyroid hormone that shuttles rapidly between the nucleus and cytoplasm. Our prior studies showed that nuclear import of TRα1 is directed by two nuclear localization signals, one in the N-terminal A/B domain and the other in the hinge domain. Here, we showed using *in vitro* nuclear import assays that TRα1 nuclear localization is temperature and energy-dependent and can be reconstituted by the addition of cytosol. In HeLa cells expressing green fluorescent protein (GFP)-tagged TRα1, knockdown of importin 7, importin β1 and importin α1 by RNA interference, or treatment with an importin β1-specific inhibitor, significantly reduced nuclear localization of TRα1, while knockdown of other importins had no effect. Coimmunoprecipitation assays confirmed that TRα1 interacts with importin 7, as well as importin β1 and the adapter importin α1, suggesting that TRα1 trafficking into the nucleus is mediated by two distinct pathways.

Key words: thyroid hormone receptor, thyroid hormone, nuclear import, importin

1. Introduction

The thyroid hormone receptor α1 (TRα1)[1] is a transcription factor in the nuclear receptor superfamily that either activates or represses transcription of thyroid hormone-responsive genes, depending on its liganded state. TRα1 carries out its function through binding target genes in the nucleus; however, our previous research has shown that TRα1 shuttles back and forth between the nucleus and the cytoplasm (Bunn et al., 2001; Grespin et al., 2008). An important aspect of nucleocytoplasmic shuttling, and for the role of TRα1 as a transcription factor, is the process by which TRα1 is imported into the nucleus from the cytoplasm by crossing the nuclear envelope. The nuclear envelope creates an intracellular compartment that enables spatial regulation of gene expression and plays a key role in signal transduction pathways, in gene activation or repression, and in the regulation of major cellular processes (Lange et al., 2010; Sekimoto and Yoneda, 2012; Stewart, 2007; Tran et al., 2014).

Nuclear proteins cross the nuclear envelope via large protein assemblages approximately 100 MDa in size called nuclear pore complexes (NPCs) (Adams and Wente, 2013). Nuclear import of small

[1] The abbreviations used are: TRα1, thyroid hormone receptor α1; TRβ1, thyroid hormone receptor β1; NPCs, nuclear pore complexes; NLS, nuclear localization signal; RNAi, RNA interference; GFP, green fluorescent protein; GST, glutathione-S-transferase; shRNA, short hairpin RNA; RT-qPCR, real-time quantitative PCR; FITC, fluorescein isothiocyanate; RRL, rabbit reticulocyte lysate; TRE, thyroid hormone response element; T_3, 3,3′,5-triiodo-L-thyronine (thyroid hormone).

molecules, including small proteins (less than 40 kDa), can occur by passive diffusion through the central channel of the NPCs; however, in most cases, both small and large proteins enter the nucleus by an energy-dependent, signal-mediated pathway (Gorlich and Kutay, 1999; Gorlich and Mattaj, 1996; Grossman et al., 2012; Stewart, 2007; Tetenbaum-Novatt and Rout, 2010). Signal-mediated transport requires soluble factors collectively called karyopherins, or importins, to facilitate translocation into the nucleus (Pemberton and Paschal, 2005; Sekimoto and Yoneda, 2012; Stewart, 2007), and also relies on an asymmetrical cellular distribution of the small GTPase Ran in either its GTP or GDP bound state. A high nuclear RanGTP concentration is required for dissociation of import complexes that have successfully passed through the NPC (Fried and Kutay, 2003; Gorlich et al., 1997; Gorlich et al., 1996; Tetenbaum-Novatt and Rout, 2010; Wente and Rout, 2010). Adding to the complexity of mechanisms for nuclear entry, a recent report suggests that an importin-dependent nuclear import pathway can be accessed by proteins with conserved ankyrin repeats (Lu et al., 2014). Importins bind to a cargo protein by recognizing a short lysine or arginine-rich amino acid motif on the cargo protein known as a nuclear localization signal (NLS). Two NLSs in TRα1 have been fully characterized: NLS-1, a classical bipartite NLS in the hinge region (Baumann et al., 2001; Casas et al., 2006; Lee and Mahdavi, 1993; Maruvada et al., 2003; Mavinakere et al., 2012; Zhu et al., 1998) and, more recently, NLS-2, a novel, monopartite NLS in the N-terminal A/B domain (Mavinakere et al., 2012).

The karyopherin-β family is responsible for the majority of nuclear transport pathways, with each member performing a distinct nuclear import, export, or bi-directional transport function (Cook et al., 2007; Macara, 2001; Strom and Weis, 2001; Xu et al., 2010). Members of this family involved in nuclear import are characterized by their ability to either bind NLS-bearing cargo directly or indirectly via an adaptor importin (Cingolani et al., 2002; Lott and Cingolani, 2011; Palmeri and Malim, 1999). Importin β1 is the best-studied member of the karyopherin-β1 family, which includes 10 other known family members that can mediate import of proteins into the nucleus (Lange et al., 2007; Mosammaparast and Pemberton, 2004; Pemberton and Paschal, 2005; Stewart, 2007; Strom and Weis, 2001). Most nuclear import occurs via direct binding of a karyopherin-β receptor to a cargo protein. In the classical nuclear import model, however, importin α acts as an adaptor protein that recognizes and binds to a specific NLS motif on the cargo, and then binds importin β1 (Lange et al., 2007; Riddick and Macara, 2005, 2007). The human genome encodes at least six importin α isoforms: α1, α3, α4, α5, α6, and α7 (Friedrich et al., 2006). Each importin α isoform is responsible for binding to and facilitating import of several different cargo proteins in conjunction with importin β1 (Cook et al., 2007; Goldfarb et al., 2004; Lange et al., 2010; Lange et al., 2007).

In the present study, we sought to characterize the general mechanism for TRα1 transport, using *in vitro* nuclear import assays. Additionally, we used RNA interference (RNAi), treatment with importazole, an importin β1-specific inhibitor, and coimmunoprecipitation assays in HeLa cells to identify which importins mediate nuclear import of TRα1. Taken together, our *in vitro* and *in vivo* data suggest that TRα1 can follow two distinct temperature and energy-dependent, signal-mediated import pathways, with importin 7, importin β1, and the adapter importin α1 acting as major players in localizing TRα1 to the nucleus.

2. Methods

2.1. *Plasmids and recombinant proteins*

pGFP-TRα1 is an expression plasmid for functional green fluorescent protein (GFP)-tagged rat TRα1 (Bunn et al., 2001), and the expression vector for enhanced GFP, EGFP-C1, was obtained from Clontech Laboratories, Inc. (Mountain View, CA). The plasmid GFP-TRβ1 encodes GFP-tagged human TRβ1 (Mavinakere et al., 2012). The GFP-glutathione-S-transferase (GST)-GFP (G3) expression vector, G3-A/BD (containing NLS-2) expression plasmid, and G3-Hinge (containing NLS-1) expression plasmid were previously described (Mavinakere et al., 2012). The plasmid hTERT-GFP was a gift from R. H.

Kehlenbach (University of Göttingen) and encodes GFP-tagged human telomerase reverse transcriptase (Frohnert et al., 2014). pGST-GFP-NLS was a gift from R. J.G. Haché (University of Ottawa) and expresses a fusion protein comprised of GST and GFP with the sequence of the simian virus 40 (SV40) T-antigen NLS (PKKKRKV) at the C terminus (Walther et al., 2003). pGEX-2T-T3Rα was a gift from M. Privalsky (University of California) and encodes GST-tagged TRα1 (Tzagarakis-Foster and Privalsky, 1998). Pre-designed SureSilencing™ short hairpin RNA (shRNA) plasmid sets, consisting of four different shRNA expression plasmids for each target mRNA, were purchased from SABioscience (Frederick, MD) for human importin α1 (KPNA2), importin α3 (KPNA4), importin α4 (KPNA3), importin α5 (KPNA1), importin α7 (KPNA6), importin β1 (KPNB1), importin 4 (IPO4), importin 5 (IPO5), importin 7 (IPO7), importin 8 (IPO8), importin 9 (IPO9), importin 11 (IPO11), importin 13 (IPO13), and a scrambled sequence negative control. The sequences of all shRNAs are provided as supplementary information (Table S1). 2xDR4-SV40-Luc was a gift from J. L. Jameson (Northwestern University), and consists of two copies of a positive, direct repeat TRE (DR+4) in the firefly luciferase vector pGL3. The plasmid pGL4.74 encodes *Renilla* luciferase (Promega, Madison, WI).

2.2. *Protein purification and FITC labeling*

Recombinant GST-tagged TRα1 was bacterially expressed and purified by binding and elution from Glutathione-Sepharose 4B resin (GE Healthcare Life Sciences, Pittsburgh, PA), as described (Grespin et al., 2008). Protein samples were analyzed by 8% or 12% SDS-PAGE and protein concentration was estimated using a NanoDrop® ND-1000 full-spectrum UV/Vis Spectrophotometer. Samples were stored at –80°C. For import assays, purified GST-TRα1 was labeled with fluorescein isothiocyanate (FITC) using a FluoReporter® Protein Labeling Kit (Life Technologies, Grand Island, NY), according to the manufacturer's instructions. The labeled sample was dialyzed against PBS overnight at 4°C, and concentrated using Micron Ultracel YM-30 Centrifugal Filter Devices (Millipore, Bedford, MA). Samples were stored at –80°C.

2.3 *Permeabilized cell nuclear import assays*

HeLa cells (American Type Culture Collection [ATCC], #CCL-2) were cultured in Minimum Essential Medium (MEM) supplemented with 10% fetal bovine serum (FBS) (Life Technologies) at 37ºC under 5% CO_2 and 98% humidity. HeLa cells were seeded on 22 mm Coverslips for Cell Growth™ (Fisher Scientific, Pittsburgh, PA) in 6 well culture dishes at a density of 2-3 x 10^5 cells per well. Sixteen to 24 h hours post-seeding the medium in each well was replaced with fresh MEM supplemented with 10% FBS. After 4 h, cells were washed 2X with 2 ml per well cold Import Buffer (20 mM HEPES, pH 7.3, 110 mM KOAc, 5 mM NaOAc, 2 mM $Mg[OAc]_2$), then permeabilized with 50 μg/ml digitonin (Calbiochem, San Diego, CA) in Import Buffer for 4 min at room temperature. Cells were rinsed 1X with 2 ml per well cold Import Buffer for 10 min, and coverslips were then inverted over 50 μl drops of Import Reaction Mix (energy regeneration system composed of 5 mM creatine phosphate, 20 U/ml creatine phosphokinase, 0.5 mM ATP, and 0.5 mM GTP in Import Buffer; 0.67 mM FITC-labeled GST-TRα1; and 25 μl rabbit reticulocyte lysate or Import Buffer) on parafilm in a moist chamber for 30 min at 30°C. For energy depletion, the energy regeneration system was replaced with apyrase (Grade VIII, 100 U/ml, Sigma-Aldrich, St. Louis, MO). Subsequently, cells were fixed in 3.7% formaldehyde (Fisher Scientific) for 10 min, followed by a 5 min wash with Import Buffer. Coverslips were mounted on slides with Fluoro-Gel II mounting medium (Electron Microscopy Sciences, Hatfield, PA) containing the DNA counter stain 4′,6-diamidino-2′-phenylindole dihydrochloride (DAPI, 0.5 μg/ml). Cells were analyzed for nuclear localization of FITC-GST-TRα1 by fluorescence microscopy.

2.4 *Importazole treatment*

HeLa cells were seeded on coverslips in 6 well culture dishes at a density of 2.0-2.5 x 10^5 cells per well. Twenty four hours post-seeding, cells were transfected with 2 μg of GFP-TRα1 or GFP-TRβ1 expression plasmid using Lipofectamine 2000 (Life Technologies). The transfection medium was replaced with fresh MEM containing 10% FBS at 5 h post-transfection. Approximately 18 h later, cells were treated for 5 h with 50 μM importazole (Calbiochem) or an equivalent volume of ethanol (vehicle control). Cells were fixed in 3.7% formaldehyde, and coverslips were mounted with Fluoro-Gel II containing DAPI (0.5 μg/ml), and then analyzed for the cellular localization of GFP-TRα1 or GFP-TRβ1 by fluorescence microscopy.

2.5 *Analysis of nuclear localization by RNA interference (RNAi)*

HeLa cells were seeded on coverslips in 6 well culture dishes at a density of 2.0-2.5 x 10^5 cells per well. Twenty four hours post-seeding, cells were cotransfected with 1 μg of the appropriate set of four target-specific or control shRNA expression plasmids and 1 μg GFP-TRα1 expression plasmid using Lipofectamine 2000. The transfection medium was replaced with fresh MEM containing 10% FBS at 8 h post-transfection. At exactly 26 h post-transfection, cells were fixed and analyzed for the cellular localization of GFP-TRα1 by fluorescence microscopy. In pilot studies, a range of post-transfection incubation times (17 h, 24 h, 26 h, and 30 h) were tested. In addition, we varied the amount of Lipofectamine 2000 and the time cells were exposed to the reagent, selected for knockdown cells with puromycin, and varied the shRNA plasmid amounts and combinations. The conditions described above showed high transfection efficiency (50-70% of cells were transfected), reduced the levels of importins in cells, and retained cell viability. Altered conditions either decreased transfection efficiency, decreased knockdown efficiency, or led to increased cell mortality. Cell mortality was assessed by visual inspection of the number of adherent cells before and after transfection, with the standard set at >60% retention.

2.6 *Validation of RNAi by real-time quantitative PCR (RT-qPCR)*

HeLa cells were seeded on 100 mm vented plates at a concentration of 6 x 10^5 cells per plate in MEM supplemented with 10% FBS. Twenty four hours post-seeding, each plate was transfected with 10 μg of a set of four target-specific or control shRNA expression plasmids using Lipofectamine 2000. The transfection medium was replaced with fresh MEM containing 10% FBS at 8 h post-transfection. At exactly 26 h post-transfection, total RNA was purified using the Aurum™ Total RNA Mini Kit (Bio-Rad, Hercules, CA), following the Spin Protocol for Cultured Mammalian Cells with a 30 min DNase I digestion. Only RNA samples with A260:A280 ratios greater than 2.0 and A260:A230 ratios greater than 1.7 were used. RNA quality and integrity was further analyzed using an RNA 6000 Pico Total RNA Assay and the Agilent 2100 BioAnalyzer's Lab-on-a-Chip technology (Santa Clara, CA).

cDNA was synthesized using SABioscience RT^2 First Strand Kit and 0.74 μg total RNA. This amount of total RNA was within the manufacturer's recommended range, and was selected to standardize all cDNA synthesis reactions. Samples for real-time quantitative PCR (RT-qPCR) were set up in a 48-well plate, using RT^2 SYBR Green/Fluorescein qPCR Master Mix (SABioscience) and SABioscience validated RT^2-qPCR primers specific for importins 7, β1, α1, α3, α4, α5, α7, or glyceraldehyde-3-phosphate dehydrogenase (GAPDH) as an internal control. No Template controls and No Reverse Transcription controls also were included for each sample. Plates were centrifuged for 90 sec at 500 x g in a Peqlab PerfectSpin plate spinner (VWR International, Radnor, PA), then analyzed using an Applied Biosystems StepOne™ Real-Time PCR machine (Life Technologies) as follows: 10 min at 95°C, then 40 cycles of 15 sec at 95°C, 35 sec at 55°C, and 30 sec at 72°C. SYBR Green fluorescence was detected and recorded during the annealing step of each cycle. A melting curve analysis was performed as a quality control measure. RT-qPCR data were analyzed by the ΔΔCt (Livak) method (Livak and Schmittgen,

2001) using StepOne™ software, and validated by manual calculation.

2.7 *Validation of RNAi by immunoblotting*

Twenty six hours post-transfection, HeLa cell protein lysates were prepared and analyzed by immunoblotting as described (Subramanian et al., 2015). Antibodies were used with the following concentrations: anti-GAPDH (Santa Cruz Biotechnology Inc, Dallas, TX), 1:5000; anti-importin β1 (Santa Cruz), 1:2000; anti-importin 4 (Santa Cruz), 1:333; anti-importin 5 (Santa Cruz), 1:10,000; anti-importin 7 (Abcam, Cambridge, MA), 1:1000; anti-importin 8 (Abcam), 1:250; anti-importin 9 (Abcam), 1:250; anti-importin 11 (Abcam), 1:333; anti-importin 13 (Santa Cruz), 1:100; anti-importin α1 (Santa Cruz), 1:2000; anti-importin α3 (Thermo Scientific), 0.2 μg/ml; horseradish peroxidase (HRP)-conjugated donkey anti-rabbit IgG (GE Healthcare Life Sciences), 1:25,000; HRP-sheep anti-mouse IgG (GE Healthcare Life Sciences), 1:25,000; or HRP-mouse anti-goat IgG (Santa Cruz Biotechnology), 1:25,000. Protein size was confirmed using Pre-Stained Kaleidoscope Protein Standards (Bio-Rad, Hercules, CA). X-ray films were quantified by scanning densitometry using NIH ImageJ software.

2.8 *Cell scoring by fluorescence microscopy and statistical analysis*

For some analyses an inverted Nikon ECLIPSE TE 2000-E fluorescence microscope (Nikon Ultraviolet Excitation: UV-2E/C filter block for DAPI visualization; Blue Excitation: B-2E/C filter block for GFP/ FITC visualization) was used with a Nikon Plan Apo 40x/0.95objective. A CoolSNAP HQ2 CCD camera (Photometrics, Tucson, AZ) and NIS-Elements AR software (Nikon) were used for image capture. For other analyses an Olympus BX60 microscope (U-MNU filter cube for DAPI; Omega Optical XF100-2 for GFP) was used with an Olympus 40xUPlanFL 40x/0.75 objective. A Cooke SenisCamQE camera and IPlab software (BD Biosciences Bioimaging Rockville, MD) were used for image capture. Images were presented using Adobe Photoshop/Illustrator.

For permeabilized cell *in vitro* nuclear import assays, the localization of FITC-GST-TRα1 was scored as "nuclear" when there was a detectable accumulation of fluorescence within the nucleus. FITC-GST-TRα1 that did not accumulate in the nucleus diffused out into the drop of Import Buffer (see Section 2.3), since the cells were permeabilized. Import assays consisted of 4 to 5 independent, biological replicates, with 200 cells scored per replicate. For RNAi experiments, the localization of GFP-TRα1 was scored in one of three categories: completely nuclear, nuclear and cytoplasmic (with distinct accumulation in the nucleus), or whole cell (with no distinct nuclear accumulation). RNAi experiments consisted of 3 independent, biological replicates, with 100 cells scored per replicate. To ensure consistency in scoring criteria, slides were randomly selected for cross-checking by other lab members. In all experiments, the integrity and morphology of the DAPI-stained nuclei was assessed visually, and only cells with intact nuclei were scored. All cell counts were performed blind, without prior knowledge of the treatment. The slides' original labels were removed and replaced with random numbers by another lab member, who made a key and kept it secure until scoring was completed and data were analyzed. For some RNAi experiments, one lab member set up the transfection and prepared slides, while another lab member scored the slides blind. Data were quantified as the percentage of cells in a given category (e.g., % of cells with a primarily nuclear distribution of TRα1) and presented as bar graphs. Bars indicate the mean percentage of cells in a given category, and error bars indicate plus or minus the standard error of the mean (± SEM). Statistical differences between two groups were determined using an unpaired Student's t test with two-tailed *P* value. Results were considered significant at $P<0.05$.

2.9. *Luciferase reporter gene assay*

Cells were seeded at 2.0×10^4 per well in a 96-well plate (PerkinElmer, Waltham, MA). Seventeen hours after seeding, cells were transiently transfected with 100 ng DNA, containing 25 ng each of

expression plasmids for GFP-TRα1, TRE (DR+4)-firefly luciferase reporter, *Renilla* luciferase internal control, scrambled shRNA control or a set of four target-specific shRNAs. Transfection medium was replaced with complete medium 8 h post-transfection. Fourteen hours post-transfection, complete medium was replaced with 100 µl MEM containing 10% charcoal-dextran stripped FBS (Life Technologies), supplemented or not with 100 nM 3,3′,5-triiodo-L-thyronine (T_3, Sigma-Aldrich). After an additional 12 h, a Dual-Glo® Luciferase Assay (Promega) was performed, according to the manufacturer's protocol, using 100 µl of reagent per well. Four independent, biologically separate replicate experiments were performed, with 8 wells assayed per treatment. Data were analyzed for statistical significance, as described in Section 2.8.

2.10 *GFP-Trap®_A coimmunoprecipitation*

HeLa cells were seeded on 100 mm vented plates at a concentration of 9 x 10^5 cells per plate in MEM supplemented with 10% FBS. Twenty four hours post-seeding, each plate was transfected with expression plasmids encoding GFP, GFP-TRα1, hTERT-GFP, GST-GFP-NLS, GFP-TRβ1, GFP-GST-GFP (G3), G3-A/BD, or G3-Hinge, using Lipofectamine 2000. After 26 h, cells were washed with ice-cold Dulbecco's phosphate-buffered saline (PBS), treated for 3 min with 0.7 ml of 0.25% trypsin (Life Technologies), collected in 1.0 ml MEM supplemented with 10% FBS, then transferred to 2.0 ml microcentrifuge tubes. Cells were washed 2X with Dulbecco's PBS, then lysed in 200 µl of Lysis Buffer (10 mM Tris-HCl, pH 7.2, 150 mM NaCl, 0.5 mM EDTA) containing 0.5% IGEPAL® (NP-40 equivalent, Sigma-Aldrich) and 1X Halt Protease Inhibitor Cocktail (Thermo Scientific). Cells were incubated for 30 min on ice, with thorough pipetting every 10 min. The lysate was cleared by centrifugation at 4°C, 16,000 x g for 10 min, and the supernatant was transferred to a new tube and diluted with 300 µl of Dilution/Washing Buffer (2 mM Tris-HCl, pH 7.5, 30 mM NaCl, 0.1 mM EDTA), containing 1X Halt Protease Inhibitor Cocktail, to yield a final concentration of 0.2% IGEPAL. GFP-trap agarose beads (GFP-Trap®_A, Chromotek GmbH, Planegg-Martinsried, Germany) were pre-equilibrated by washing 3X with Dilution/Washing Buffer, then 20 µl were added to each diluted supernatant. After 2.5 h of incubation at 4°C with end-over-end rotation, beads were centrifuged at 4°C, 3000 x g for 4 min. A 50 µl sample of the supernatant (unbound proteins) was collected and resuspended with an equal volume of 2X Sample Buffer (2% SDS, 10% glycerol, 250 mM Tris-HCl, pH 6.8, 0.01% bromophenol blue, 20 mM DTT). The beads were washed 3X with 100 µl Dilution/Washing Buffer lacking IGEPAL, then resuspended in 100 µl of 2X Sample Buffer. Samples of unbound and bound proteins (20 µl) were analyzed by immunoblotting (see Section 2.7), using SuperSignal™ West Femto Maximum Sensitivity Substrate (Thermo Scientific). Antibodies were used at the following concentrations: anti-GFP (Santa Cruz), 1:2000; anti-importin 4 (Abcam), 1:1250; anti-importin 7 (Abcam), 1:1000; anti-importin β1 (Santa Cruz), 1:1000; anti-importin α1 (Abcam), 1:1000; horseradish peroxidase (HRP)-conjugated donkey anti-rabbit IgG (GE Healthcare Life Sciences), 1:25,000 or 1:33,000.

3. Results

3.1. *TRα1 follows a signal-mediated import pathway in HeLa cells*

Our prior studies showed that TRα1 follows both signal-mediated and passive diffusion import pathways in *Xenopus* oocytes (Bunn et al., 2001). We also showed that there is an energy-requiring step in the nuclear retention or nuclear export process in mammalian cells; however, we did not address the import mechanism in mammalian cells. Given the specialized nature of these amphibian oocytes, it was of interest to determine whether TRα1 would follow a signal-mediated import pathway in mammalian cells. To this end, permeabilized HeLa (human) cell *in vitro* nuclear import assays (Adam et al., 1990) were used to address this question.

To test whether soluble factors are required for nuclear entry of TRα1, FITC-labeled recombinant

GST-TRα1 was used for import assays in the presence or absence of rabbit reticulocyte lysate (RRL), as a cytosol replacement. In the presence of RRL, TRα1 was able to translocate into the nucleus from its starting point in the cytoplasm. After 30 min incubation at 30°C, on average 61% of cells showed a predominantly nuclear localization of TRα1. In the absence of RRL, TRα1 showed a significantly different localization pattern (Fig. 1, A and B; P=0.00001); the receptor did not accumulate in the nucleus, and formed aggregates or showed fluorescent staining of the nuclear periphery, an indicator of binding at the NPC without subsequent translocation (Newmeyer and Forbes, 1988). On average, TRα1 was only localized to the nucleus in 11% of cells .

Next, we sought to determine whether TRα1 import was temperature-dependent. Chilling has been shown to abolish active transport while only marginally affecting passive transport (Breeuwer and Goldfarb, 1990; Freedman and Yamamoto, 2004). However, given that FITC-GST-TRα1 is 73 kDa in size, this likely would preclude rapid passive diffusion through the NPCs regardless of temperature. Import reactions were incubated at 4°C for 30 min. Nuclear import of FITC-GST-TRα1 was significantly inhibited in chilled cells (Fig. 1, A and B*; P*=0.007); on average, only 26% of cells showed nuclear accumulation of TRα1. Nuclear import could be fully restored, however, by further incubation at 30°C (P=0.584). Reversible inhibition suggests that chilling blocked TRα1 import by inhibiting specific transport components, rather than by preventing import by way of non-specific cellular damage (Bunn et al., 2001).

To further characterize the energy requirements for nuclear import of TRα1 in permeabilized HeLa cells, the effects of energy depletion were studied by apyrase treatment, which depletes cellular ATP and GTP (Bunn et al., 2001). Import assays were performed in the presence of RRL, as a cytosol replacement, and in the presence of an energy regeneration system or apyrase (Fig. 1, A and B). Incubation at 30°C for 30 min with apyrase significantly inhibited nuclear accumulation of FITC-GST-TRα1 (P=0.025). On average, only 40% of cells showed nuclear localization of TRα1, compared to reactions containing RRL and an energy regeneration system in which TRα1 was localized primarily to the nucleus in 61% of cells. However, TRα1 import in the presence of apyrase was not inhibited to the same extent as import in the absence of RRL, where only 11% of cells showed nuclear accumulation of TRα1.

Soluble factor dependence, chilling inhibition, and energy dependence are commonly used criteria when establishing a signal-mediated import pathway (Carazo et al., 2012; Dhanoya et al., 2013; Umemoto and Fujiki, 2012; Vazquez-Iglesias et al., 2009, 2012), and thus demonstrate a requirement for signal-mediated nuclear import of TRα1 in HeLa cells. To begin to characterize the soluble components required for nuclear localization of TRα1, we turned to an *in vivo* approach to evaluate the role of a panel of importins in promoting TRα1 nuclear import in HeLa cells.

3.2 *Knockdown of importin β1 and importin 7 reduces TRα1 nuclear localization*

RNAi is a powerful tool for knockdown of the expression of a specific gene *in vivo* by targeting its mRNA for degradation. We chose to use importin-specific shRNA expression plasmids, to ensure sustained depletion of protein levels. Since TRα1 is primarily nuclear at steady-state, but shuttles between the nucleus and the cytosol, effective knockdown of an essential import factor would be predicted to result in a shift to a more cytoplasmic distribution of TRα1 over time. It is important to note, however, that it was not expected that cells would ever show a fully cytoplasmic distribution of TRα1 for a number of reasons. First, RNAi leaves a residual portion of target mRNA and protein in cells. Second, a wholly cytoplasmic distribution would depend on the complete export of all nuclear TRα1, which is unlikely as it is strongly retained in the nucleus by interaction with target genes.

Although the classical importin α1/β1 import pathway is widely used by nuclear proteins, and was thus a priority to investigate, other import pathways exist. Of particular interest for this study, importin 7 mediates nuclear import of a diversity of cargos including the glucocorticoid receptor (Chook and Suel, 2011; Strom and Weis, 2001). Thus, we also evaluated importin 7 for its role in promoting TRα1 nuclear

localization. First, shRNA-induced knockdown of importin β1 and importin 7 mRNA was validated by RT-qPCR and protein levels were quantified by immunoblot analysis. Twenty six hours post-transfection with shRNA expression plasmids, the levels of importin β1 and importin 7 mRNA in HeLa cells were reduced to 21% and 19%, respectively, relative to the control shRNA (set to 100%) (Fig. 2A). Importin β1 and importin 7 protein levels were reduced to 56% and 49%, respectively, relative to the scrambled control (Fig. 2B), indicating the efficacy of the RNAi system. Control immunoblots also confirmed the specificity of shRNA-mediated knockdown of importin 7, importin β1, and importin α1 (see Section 3.3); shRNA-targeting a particular importin did not exhibit any cross-inhibition of another importin (Fig. 2C).

Next, in a parallel experiment, the effect of importin β1 and importin 7 knockdown on the cellular localization of GFP-TRα1 at 26 h post-transfection was assessed by fluorescence microscopy. Knockdown of importin β1 resulted in a significant shift in localization of TRα1 to a more cytoplasmic distribution (P=0.002); on average only 72% of cells showed TRα1 primarily localized to the nucleus, compared with 86% of cells in the presence of control shRNA (Fig. 3, A and B).

Knockdown of importin 7 caused a significant shift in localization of TRα1 to a more cytoplasmic distribution (Fig. 3, A and B; P=0.0001); on average, only 66% of cells showed TRα1 localized to the nucleus, with a concomitant increase in the number of cells with a whole cell distribution of TRα1. In addition, many of these cells were marked by numerous small cytoplasmic or perinuclear aggregates of TRα1. Such an accumulation of foci was typically not observed upon knockdown of the other importins tested. Interestingly, knockdown of importin 7 has been shown to alter nucleolar morphology, resulting in a more punctate distribution of fibrillarin (Golomb et al., 2012). Taken together our findings suggest that both importin β1 and importin 7 play key roles in promoting nuclear localization of TRα1 *in vivo*.

3.3. *Knockdown of importin α1 reduces TRα1 nuclear localization*

In an effort to further characterize additional importins playing a role in the signal-mediated import pathway, the adaptor importins α1, α3, α4, α5, and α7 were screened as well. Importin α6 was excluded from the analysis because its expression appears to be limited to the testis (Chook and Suel, 2011). These importins are known to mediate import in conjunction with importin β1 in the classical nuclear import pathway. We were unable to achieve sufficient knockdown of the levels of importin α5 mRNA; levels only were reduced to 68% relative to the control shRNA with the set of four shRNA expression plasmids used. Thus, further analysis of this adaptor protein was not performed. In contrast, levels of importin α1 mRNA were knocked down to 23% of control levels, while levels of importin α3, α4, and α7 mRNA were knocked down to 5%, 16%, and 8%, respectively (Fig. 4A). Accordingly, levels of importin α1, α3, and α7 proteins were knocked down to 55%, 49%, and 49%, respectively, compared with the scrambled control (Fig. 4B). At the time this study was performed, no antibodies were available for importin α4, so we were only able to assess knockdown via RT-qPCR in this case.

Knockdown of importin α1 resulted in a significant shift of TRα1 towards a more cytoplasmic distribution (Fig. 4, C and D*;* P=0.025); on average, only 71% of cells showed a primarily nuclear localization of TRα1, compared to 86% of cells in the shRNA control (Fig. 4, C and D). There was no significant change in nuclear localization in cells depleted of importin α3 (P=0.190), importin α4 (P=0.425) and importin α7 (P=0.721) (Fig. 4D), although results with importin α7 were highly variable between replicates. These findings suggest that importin α1 is the main adaptor acting with importin β1 for nuclear localization of TRα1.

We thought that dual knockdown with combinations of shRNA against importin α1/importin β1 or importin 7/importin β1 might have a greater impact than single knockdowns. However, these combinations did not result in further shifts in the distribution pattern of TRα1, although this could well be due to increased cell mortality. These importins are required for nuclear localization of many other proteins involved in essential cell processes. In addition, since cellular microRNAs (miRNAs) regulate the expression of hundreds of genes, saturation of the RNAi pathway with exogenous shRNA also could

contribute to loss of cell viability (Castanotto and Rossi, 2009; Scherr and Eder, 2007). Further, it is likely that the primarily nuclear location of TRα1 at steady-state limits how much the distribution pattern can be altered over the time course of an experiment. We found that extending the time course for knockdown of importins beyond 26 h post-transfection caused a marked decrease in cell viability, in particular for importin β1. This is consistent with a report that reduced levels of importin β1 are more harmful to a cell than reduction in the levels of importin α (Quensel et al., 2004).

3.4. *Nuclear import of TRα1 and TRβ1 is inhibited by importazole*

To provide further evidence that importin β1 plays a role in mediating TRα1 nuclear localization, we made use of importazole, a small molecule inhibitor of this pathway. Importazole specifically blocks importin β1-mediated nuclear import, without disrupting transportin-mediated nuclear import or CRM1-mediated nuclear export (Soderholm et al., 2011). Treatment of GFP-TRα1-expressing HeLa cells with importazole resulted in a 16% reduction in nuclear localization of TRα1 compared with cells treated with the vehicle control (P=0.000001) (Fig. 5A), providing further support for a central role of importin β1 in TRα1 nuclear localization.

The nuclear localization signal, NLS-1, in the hinge domain of TRα1 is conserved in the other major TR subtype, the thyroid hormone receptor β1 (TRβ1); however, NLS-2 in the A/B domain of TRα1 is absent from TRβ1 (Mavinakere et al., 2012). TRβ1 typically has a small cytosolic population at steady-state, suggesting that its distinct distribution pattern may reflect an altered balance of nuclear import and nuclear export activity, relative to TRα1. We thus included TRβ1 in our analysis to provide a means of teasing apart whether importin 7 and the importin α1/β1 heterodimer interact selectively with one or the other NLS. Treatment of GFP-TRβ1-expressing HeLa cells with importazole resulted in a 12% reduction in nuclear localization of TRβ1 compared with cells treated with the vehicle control (P=0.001) (Fig. 5B), suggesting that importin β1 plays a role in TRβ1 nuclear localization, and that the interaction is mediated by the hinge domain NLS-1.

3.5. *Analysis of other import pathways*

Having shown that TRα1 localization is influenced by knockdown of importin 7, importin β1, and importin α1, the question still remained of whether additional pathways for nuclear entry are followed by TRα1. To determine whether other importins play a role in TRα1 nuclear localization, we screened the remainder of the well-characterized importins (Chook and Suel, 2011; Kimura and Imamoto, 2014). Given the structural similarity between importin 4 and importin β1 (Pradeepa et al., 2008), and that importin 4 mediates import of another member of the nuclear receptor superfamily, the vitamin D receptor (Miyauchi et al., 2005), we predicted that importin 4 might also influence TRα1 accumulation. Many cargoes that are primarily imported by importin 4 also use importin 5 as an alternative pathway (Chook and Suel, 2011). Thus, we predicted that if importin 4 was a mediator of TRα1 import, then knockdown of importin 5 would have no effect on TRα1 nuclear localization when importin 4 was present in the cell. Importin 8 is structurally similar to importin 7 (Chook and Suel, 2011; Weinmann et al., 2009), so it was also conceivable that this importin could play a role in TRα1 import. In addition, importin 13 has been shown to be one of the importins that mediates glucocorticoid receptor import (Tao et al., 2006), so importin 13 also appeared to be a likely candidate. Importin 9 imports some ribosomal proteins (Jakel et al., 2002) and nuclear actin (Kimura and Imamoto, 2014), while importin 11 imports the ubiquitin-conjugating enzyme, UbcM2 (Plafker and Macara, 2000). No role has yet been reported for these karyopherins, or for transportins 1 and 2 (Twyffels et al., 2014), in import of nuclear receptors, so they were considered less likely candidates. In a separate study focused on TRα1 nuclear export pathways, we confirmed that transportins 1 and 2 are not involved in nuclear import (or export) of TRα1 (Subramanian et al., 2015).

Efficacy of knockdown was assessed by immunoblotting (Fig. 6A), with levels of knockdown relative to the scrambled control as follows: importin 4, 61%; importin 5, 63%; importin 8, 65%; importin 9, 51%, importin 11, 55%, and importin 13, 59%. There was no significant change in nuclear localization of TRα1 in cells depleted of importin 4 (P=0.99), importin 5 (P=0.34), importin 8 (P=0.60), importin 9 (P=0.89), importin 11 (P=0.55), and 13 (P=0.70), relative to the scrambled control (Fig. 6, B and C). Taken together, these data indicate that importins 4, 5, 8, 9, 11, and 13 either play no role in localizing TR to the nucleus, or are minor, nonessential mediators of nuclear localization, relative to importin 7 and the importin α1/β1 heterodimer.

Given that TRα1 is a transcription factor that either represses or stimulates expression of T_3-responsive genes, we sought to ascertain whether the cytoplasmic shift in TRα1's distribution resulting from knockdown of importins 7, β1, or α1 would reduce TRα1-mediated gene expression to a comparable extent. A firefly luciferase reporter gene under the positive control of a thyroid hormone response element (TRE) was used to examine ligand-dependent transactivation by GFP-TRα1 (Fig. 7), in the presence of shRNAs specific for importin 4 (no cytoplasmic shift), importin β1, importin 7, or importin α1. Fold stimulation in the presence of importin-specific shRNAs was not significantly different compared with fold stimulation in the presence of the scrambled shRNA control (importin 4, P=0.62; importin β1, P=0.09; importin 7; P=0.24; importin α1, P=0.27), indicating that under these conditions a reduction in nuclear TRα1 of 14-20% does not have a measurable impact on reporter gene expression. As noted earlier, these importins are required for nuclear localization of many other proteins involved in transcriptional regulation. Importin knockdown is not specific for TRα1 import and, thus, may impact transcriptional output in complex, unanticipated ways.

3.6. *Importin 7, importin β1, and importin α1 interact with TRα1*

Since knockdown of importin 7, importin β1, and importin α1 leads to a significant shift in TRα1 localization to a more cytoplasmic distribution, we sought to ascertain whether this shift correlates with protein-protein interactions. To confirm that these importins interact with TRα1 *in vivo*, we performed "GFP-trap" coimmunoprecipitation assays on lysates from HeLa cells that had been transfected with expression plasmids for GFP, GFP-TRα1, GFP-TRβ1, or GST-GFP-NLS, a fusion protein containing the classical SV40 NLS (Lange et al., 2010; Walther et al., 2003) (Fig. 8). We confirmed that GFP, GFP-TRα1, GFP-TRβ1, and GST-GFP-NLS were all successfully immunoprecipitated by the GFP-trap assay, by immunoblot analysis of immunoprecipitate samples with anti-GFP antibodies (Fig. 8A). Samples of unbound proteins (immunosupernatant) and bound proteins (immunoprecipitates) were also analyzed for the presence of different importins on separate blots using importin-specific antibodies (Fig. 8B). Endogenous importin β1, importin α1, and importin 7 were coimmunoprecipitated (trapped) with GFP-TRα1, but not with GFP, indicating that these transport factors specifically interact with TRα1 *in vivo*, either as part of a complex (e.g., importin β1 via the adaptor importin α1) or separately. In contrast, GST-GFP-NLS trapped importin β1 and importin α1, but did not interact with importin 7 (Fig. 6B). As a positive control for the method we also confirmed that importin 7 coimmunoprecipitated with hTERT-GFP (data not shown), as this interaction had been reported previously (Frohnert et al., 2014). Finally, we used importin 4 as a negative control, since knockdown of cellular levels of importin 4 had no effect on TRα1 localization. As expected, importin 4 was not trapped by GFP, GFP-TRα1, or GST-GFP-NLS (Fig. 8B), further validating the RNAi screen as a predictive tool for assessing the role of different importins in mediating nuclear import.

To examine whether importin 7 and the importin α1/β1 heterodimer interact selectively with NLS-1 (hinge domain) or NLS-2 (A/B domain) in TRα1, we used two different approaches. First, we investigated whether TRβ1, which only contains NLS-1, interacts with these importins, using the GFP-trap assay. Samples of unbound proteins (immunosupernatant) from GFP-TRβ1-expressing HeLa cell lysates and bound proteins (immunoprecipitates) were analyzed for the presence of "trapped" importins

by immunoblotting using importin-specific antibodies (Fig. 8C). Endogenous importin β1 and the adaptor importin α1 were coimmunoprecipitated with GFP-TRβ1, but not with GFP (in some assays there was a trace amount of non-specific trapping of importins by GFP), indicating that these transport factors specifically interact with TRβ1 *in vivo*. In contrast, importin 7 did not show interaction above background levels with GFP-TRβ1 (Fig. 8C).

In a second approach, we investigated whether the TRα1 hinge domain or the A/B domain alone, fused with GFP-GST-GFP (G3) interacted with these importins. We have previously shown that G3-Hinge has a predominantly nuclear localization, comparable to full-length TRα1, whereas only around 50% of cells show a predominantly nuclear localization of G3-A/BD (Mavinakere et al., 2012), indicating that NLS-2 is less efficient in facilitating nuclear import in isolation. HeLa cells were transfected with expression plasmids for G3, G3-Hinge, or G3-A/BD and immunoprecipitated by the GFP-trap assay. Samples of unbound proteins and bound proteins were analyzed for the presence of G3 fusion proteins with GFP-specific antibodies (data not shown), and with the different importins on separate blots using importin-specific antibodies (Fig. 8D). Endogenous importin β1 and importin α1 were coimmunoprecipitated (trapped) with both G3-Hinge and G3-A/BD, indicating that these transport factors specifically interact with NLS-1 and NLS-2 *in vivo*. In contrast, no consistent interaction above background levels was observed between importin 7 and G3-Hinge or G3-A/BD (Fig. 8D).

Taken together, we conclude from these results that TRα1 nuclear import is facilitated by importin 7, likely through interactions with NLS-2, and importin β1 and the adapter importin α1 interacting with NLS-1 and NLS-2, while TRβ1 nuclear import is facilitated by importin α1/β1 interacting with NLS-1. Further studies with purified recombinant proteins *in vitro* will be required to confirm this model, since we were not able to show direct interaction between importin 7 and NLS-2 in this study. When taken out of the context of the full protein, the A/B domain NLS-2 may not be exposed in a way that promotes stable binding under the conditions of the GFP-trap assay.

4. Discussion

Our interest for many years has been in the complex mechanisms regulating the subcellular distribution of TRα1. The emerging picture is one of a finely balanced, dynamic process in which TRα1 shuttles between the nucleus and cytoplasm. Here, we have further investigated the pathway by which TRα1 enters the nucleus, using *in vitro* nuclear import assays, importin-specific shRNAs and a small molecule inhibitor of importin β1, in combination with localization assays in transfected cells and coimmunoprecipitation assays to confirm interacting partners. The results of this research show that TRα1 can enter the nucleus by more than one pathway; both importin 7 and the classical importin α1/β1 heterodimer mediate TRα1 nuclear import.

The use of more than one pathway by individual cargos is not without precedent. A striking example is the human immunodeficiency virus type 1 Rev protein which binds specifically to importin β1, transportin 1, importin 5, and importin 7 (Arnold et al., 2006). Importin 7 is a notably versatile karyopherin and often plays a shared role with other karypherin-β family members in importing cargo, ranging from ribosomal proteins (Jakel and Gorlich, 1998) and histones (Baake et al., 2001; Muhlhausser et al., 2001) to transcription factors, such as c-Jun (Waldmann et al., 2007) and Smad3 (Chuderland et al., 2008). Adding to its versatility, importin 7 can mediate import either as a monomer or as an importin 7/importin β1 heterodimer (Chook and Suel, 2011).

There is ample evidence that other members of the nuclear receptor superfamily are imported via multiple pathways. For example, the glucocorticoid receptor (GR) contains two NLSs, NL1 and NL2, each of which has been shown by *in vitro* binding assays to interact directly with importin 7 and importin 8, but only NL1 was able to bind the importin α/β heterodimer. Further, only importin 7 and the importin α/β heterodimer were able to import an NL1-containing fragment of GR in an *in vitro* import assay (Freedman and Yamamoto, 2004). In addition, GST pull-down and coimmunoprecipitation assays have

shown that importin 13 also binds GR, and silencing of importin 13 by RNAi inhibits nuclear import of GR (Tao et al., 2006). The androgen receptor also contains two NLSs and import is mediated via two pathways: one that is dependent on importin α1/β1, and one that is importin α1/β1-independent (Cutress et al., 2008; Kaku et al., 2008).

The six identified mammalian importin α adaptors are ubiquitously expressed, with the exception of testis-specific importin α6 (Kelley et al., 2010; Kohler et al., 1999). Although interchangeable for many substrates *in vitro,* there are reports of preferential use of specific importin α adapters *in vivo;* for example, for NF-κB (Fagerlund et al., 2005), STAT3 (Liu et al., 2005), the Ran guanine nucleotide exchange factor, RCC1 (Friedrich et al., 2006; Quensel et al., 2004), and STAT5a (Shin and Reich, 2013). Our findings suggest that only importin α1 plays a key role in mediating import of TRα1, adding to the preferential use of this adaptor *in vivo*.

The critical role of nuclear import as a control point for modulating thyroid hormone-responsive gene expression is apparent, but the physiological significance of multiple import pathways remains to be determined. Our prior studies have shown that the hinge region of TRα1 contains NLS-1, a classical, bipartite NLS (^{130}KRVAKRKLIEQNRERRRK^{147}; Mavinakere et al., 2012). Data presented here indicate that import from this classical NLS is mediated by importins α1 and β1 acting together. TRα1 also harbors a second, non-classical NLS, NLS-2, in the N-terminal A/B domain (^{22}PDGKRKRK^{29}; Mavinakere et al., 2012). TRβ1 only harbors NLS-1 (Mavinakere et al., 2012) and, as shown here, does not interact with importin 7. By default, this suggests that the novel monopartite NLS-1 in TRα1 provides the signal for use of an alternative pathway for nuclear entry facilitated by importin 7, at a different time, or in a cooperative fashion with the classical NLS to enable complete, efficient TRα1 import. Additional analyses of protein-protein interactions by *in vitro* binding assays with purified proteins should help to identify and clarify whether this NLS interacts directly with an importin 7 monomer, or potentially with an importin 7/importin β1 heterodimer , and will allow fuller elucidation of how multiple pathways serve to regulate nuclear entry in response to cell-specific signals.

Acknowledgments

We wish to thank Lidia Epp for excellent technical assistance with RT-qPCR, and Christopher Seibert for performing preliminary siRNA studies as part of his Senior Honors Thesis at the College of William & Mary. This work was supported in part by National Institutes of Health grant 2R15DK058028-03 and National Science Foundation grant MCB 1120513 (to L.A.A.), and grants from the Charles Center at the College of William and Mary (to Y.D. and E.L.M.)

References

Adam, S.A., Marr, R.S., and Gerace, L. (1990). Nuclear protein import in permeabilized mammalian cells requires soluble cytoplasmic factors. J Cell Biol *111*, 807-816.

Adams, R.L., and Wente, S.R. (2013). Uncovering nuclear pore complexity with innovation. Cell *152*, 1218-1221.

Arnold, M., Nath, A., Hauber, J., and Kehlenbach, R.H. (2006). Multiple importins function as nuclear transport receptors for the Rev protein of human immunodeficiency virus type 1. J Biol Chem *281*, 20883-20890.

Baake, M., Bauerle, M., Doenecke, D., and Albig, W. (2001). Core histones and linker histones are imported into the nucleus by different pathways. Eur J Cell Biol *80*, 669-677.

Baumann, C.T., Maruvada, P., Hager, G.L., and Yen, P.M. (2001). Nuclear cytoplasmic shuttling by thyroid hormone receptors. J Biol Chem *276*, 11237-11245.

Breeuwer, M., and Goldfarb, D.S. (1990). Facilitated nuclear transport of histone H1 and other small nucleophilic proteins. Cell *60*, 999-1008.

Bunn, C.F., Neidig, J.A., Freidinger, K.E., Stankiewicz, T.A., Weaver, B.S., McGrew, J., and Allison, L.A. (2001). Nucleocytoplasmic shuttling of the thyroid hormone receptor α. Mol Endocrinol *15*, 512-533.

Carazo, A., Levin, J., Casas, F., Seyer, P., Grandemange, S., Busson, M., Pessemesse, L., Wrutniak-Cabello, C., and Cabello, G. (2012). Protein sequences involved in the mitochondrial import of the 3,5,3'-L-triiodothyronine receptor p43. J Cell Physiol *227*, 3768-3777.

Casas, F., Busson, M., Grandemange, S., Seyer, P., Carazo, A., Pessemesse, L., Wrutniak-Cabello, C., and Cabello, G. (2006). Characterization of a novel thyroid hormone receptor α variant involved in the regulation of myoblast differentiation. Mol Endocrinol *20*, 749-763.

Castanotto, D., and Rossi, J.J. (2009). The promises and pitfalls of RNA-interference-based therapeutics. Nature *457*, 426-433.

Chook, Y.M., and Suel, K.E. (2011). Nuclear import by karyopherin-βs: recognition and inhibition. Biochim Biophys Acta *1813*, 1593-1606.

Chuderland, D., Konson, A., and Seger, R. (2008). Identification and characterization of a general nuclear translocation signal in signaling proteins. Mol Cell *31*, 850-861.

Cingolani, G., Bednenko, J., Gillespie, M.T., and Gerace, L. (2002). Molecular basis for the recognition of a nonclassical nuclear localization signal by importin β. Mol Cell *10*, 1345-1353.

Cook, A., Bono, F., Jinek, M., and Conti, E. (2007). Structural biology of nucleocytoplasmic transport. Annu Rev Biochem *76*, 647-671.

Cutress, M.L., Whitaker, H.C., Mills, I.G., Stewart, M., and Neal, D.E. (2008). Structural basis for the nuclear import of the human androgen receptor. J Cell Sci *121*, 957-968.

Dhanoya, A., Wang, T., Keshavarz-Moore, E., Fassati, A., and Chain, B.M. (2013). Importin-7 mediates nuclear trafficking of DNA in mammalian cells. Traffic *14*, 165-175.

Fagerlund, R., Kinnunen, L., Kohler, M., Julkunen, I., and Melen, K. (2005). NF-κB is transported into the nucleus by importin α3 and importin α4. J Biol Chem *280*, 15942-15951.

Freedman, N.D., and Yamamoto, K.R. (2004). Importin 7 and importin α/importin β are nuclear import receptors for the glucocorticoid receptor. Mol Biol Cell *15*, 2276-2286.

Fried, H., and Kutay, U. (2003). Nucleocytoplasmic transport: taking an inventory. Cell Mol Life Sci *60*, 1659-1688.

Friedrich, B., Quensel, C., Sommer, T., Hartmann, E., and Kohler, M. (2006). Nuclear localization signal and protein context both mediate importin α specificity of nuclear import substrates. Mol Cell Biol *26*, 8697-8709.

Frohnert, C., Hutten, S., Walde, S., Nath, A., and Kehlenbach, R.H. (2014). Importin 7 and Nup358 promote nuclear import of the protein component of human telomerase. PloS One *9*, e88887.

Goldfarb, D.S., Corbett, A.H., Mason, D.A., Harreman, M.T., and Adam, S.A. (2004). Importin α: a multipurpose nuclear-transport receptor. Trends Cell Biol *14*, 505-514.

Golomb, L., Bublik, D.R., Wilder, S., Nevo, R., Kiss, V., Grabusic, K., Volarevic, S., and Oren, M. (2012). Importin 7 and exportin 1 link c-Myc and p53 to regulation of ribosomal biogenesis. Mol Cell *45*, 222-232.

Gorlich, D., Dabrowski, M., Bischoff, F.R., Kutay, U., Bork, P., Hartmann, E., Prehn, S., and Izaurralde, E. (1997). A novel class of RanGTP binding proteins. J Cell Biol *138*, 65-80.

Gorlich, D., and Kutay, U. (1999). Transport between the cell nucleus and the cytoplasm. Annu Rev Cell Dev Biol *15*, 607-660.

Gorlich, D., and Mattaj, I.W. (1996). Nucleocytoplasmic transport. Science *271*, 1513-1518.

Gorlich, D., Pante, N., Kutay, U., Aebi, U., and Bischoff, F.R. (1996). Identification of different roles for RanGDP and RanGTP in nuclear protein import. EMBO J *15*, 5584-5594.

Grespin, M.E., Bonamy, G.M., Roggero, V.R., Cameron, N.G., Adam, L.E., Atchison, A.P., Fratto, V.M., and Allison, L.A. (2008). Thyroid hormone receptor α1 follows a cooperative CRM1/calreticulin-mediated nuclear export pathway. J Biol Chem *283*, 25576-25588.

Grossman, E., Medalia, O., and Zwerger, M. (2012). Functional architecture of the nuclear pore complex. Annu Rev Biophys *41*, 557-584.

Jakel, S., and Gorlich, D. (1998). Importin β, transportin, RanBP5 and RanBP7 mediate nuclear import of ribosomal proteins in mammalian cells. EMBO J *17*, 4491-4502.

Jakel, S., Mingot, J.M., Schwarzmaier, P., Hartmann, E., and Gorlich, D. (2002). Importins fulfil a dual function as nuclear import receptors and cytoplasmic chaperones for exposed basic domains. EMBO J *21*, 377-386.

Kaku, N., Matsuda, K., Tsujimura, A., and Kawata, M. (2008). Characterization of nuclear import of the domain-specific androgen receptor in association with the importin α/β and Ran-guanosine 5'-triphosphate systems. Endocrinol *149*, 3960-3969.

Kelley, J.B., Talley, A.M., Spencer, A., Gioeli, D., and Paschal, B.M. (2010). Karyopherin α7 (KPNA7), a divergent member of the importin α family of nuclear import receptors. BMC Cell Biol *11*, 63.

Kimura, M., and Imamoto, N. (2014). Biological significance of the importin-β family-dependent nucleocytoplasmic transport pathways. Traffic *15*, 727-748.

Kohler, M., Speck, C., Christiansen, M., Bischoff, F.R., Prehn, S., Haller, H., Gorlich, D., and Hartmann, E. (1999). Evidence for distinct substrate specificities of importin α family members in nuclear protein import. Mol Cell Biol *19*, 7782-7791.

Lange, A., McLane, L.M., Mills, R.E., Devine, S.E., and Corbett, A.H. (2010). Expanding the definition of the classical bipartite nuclear localization signal. Traffic *11*, 311-323.

Lange, A., Mills, R.E., Lange, C.J., Stewart, M., Devine, S.E., and Corbett, A.H. (2007). Classical nuclear localization signals: definition, function, and interaction with importin α. J Biol Chem *282*, 5101-5105.

Lee, Y., and Mahdavi, V. (1993). The D domain of the thyroid hormone receptor α 1 specifies positive and negative transcriptional regulation functions. J Biol Chem *268* 2021-2028.

Liu, L., McBride, K.M., and Reich, N.C. (2005). STAT3 nuclear import is independent of tyrosine phosphorylation and mediated by importin-α 3. Proc Natl Acad Sci USA *102*, 8150-8155.

Livak, K.J., and Schmittgen, T.D. (2001). Analysis of relative gene expression data using real-time quantitative PCR and the 2(-Δ Δ C(T)) method. Methods *25*, 402-408.

Lott, K., and Cingolani, G. (2011). The importin β binding domain as a master regulator of nucleocytoplasmic transport. Biochim Biophys Acta *1813*, 1578-1592.

Lu, M., Zak, J., Chen, S., Sanchez-Pulido, L., Severson, D.T., Endicott, J., Ponting, C.P., Schofield, C.J., and Lu, X. (2014). A code for RanGDP binding in ankyrin repeats defines a nuclear import pathway. Cell *157*, 1130-1145.

Macara, I.G. (2001). Transport into and out of the nucleus. Microbiol Mol Biol Rev *65*, 570-594.

Maruvada, P., Baumann, C.T., Hager, G.L., and Yen, P.M. (2003). Dynamic shuttling and intranuclear mobility of nuclear hormone receptors. J Biol Chem *278*, 12425-12432.

Mavinakere, M.S., Powers, J.M., Subramanian, K.S., Roggero, V.R., and Allison, L.A. (2012). Multiple novel signals mediate thyroid hormone receptor nuclear import and export. J Biol Chem *287*, 31280-31297.

Miyauchi, Y., Michigami, T., Sakaguchi, N., Sekimoto, T., Yoneda, Y., Pike, J.W., Yamagata, M., and Ozono, K. (2005). Importin 4 is responsible for ligand-independent nuclear translocation of vitamin D receptor. J Biol Chem *280*, 40901-40908.

Mosammaparast, N., and Pemberton, L.F. (2004). Karyopherins: from nuclear-transport mediators to nuclear-function regulators. Trends Cell Biol *14*, 547-556.

Muhlhausser, P., Muller, E.C., Otto, A., and Kutay, U. (2001). Multiple pathways contribute to nuclear import of core histones. EMBO Rep *2*, 690-696.

Newmeyer, D.D., and Forbes, D.J. (1988) Nuclear import can be separated into distinct steps in vitro: nuclear pore binding and translocation. Cell *52*, 641-653.

Palmeri, D., and Malim, M.H. (1999). Importin β can mediate the nuclear import of an arginine-rich nuclear localization signal in the absence of importin α. Mol Cell Biol *19*, 1218-1225.

Pemberton, L.F., and Paschal, B.M. (2005). Mechanisms of receptor-mediated nuclear import and nuclear export. Traffic *6*, 187-198.
Plafker, S.M., and Macara, I.G. (2000). Importin-11, a nuclear import receptor for the ubiquitin-conjugating enzyme, UbcM2. EMBO J *19*, 5502-5513.
Pradeepa, M.M., Manjunatha, S., Sathish, V., Agrawal, S., and Rao, M.R. (2008). Involvement of importin-4 in the transport of transition protein 2 into the spermatid nucleus. Mol Cell Biol *28*, 4331-4341.
Quensel, C., Friedrich, B., Sommer, T., Hartmann, E., and Kohler, M. (2004). In vivo analysis of importin α proteins reveals cellular proliferation inhibition and substrate specificity. Mol Cell Biol *24*, 10246-10255.
Riddick, G., and Macara, I.G. (2005). A systems analysis of importin-α-β mediated nuclear protein import. J Cell Biol *168*, 1027-1038.
Riddick, G., and Macara, I.G. (2007). The adapter importin-α provides flexible control of nuclear import at the expense of efficiency. Mol Syst Biol *3*, 118.
Scherr, M., and Eder, M. (2007). Gene silencing by small regulatory RNAs in mammalian cells. Cell Cycle *6*, 444-449.
Sekimoto, T., and Yoneda, Y. (2012). Intrinsic and extrinsic negative regulators of nuclear protein transport processes. Genes Cells *17*, 525-535.
Shin, H.Y., and Reich, N.C. (2013). Dynamic trafficking of STAT5 depends on an unconventional nuclear localization signal. J Cell Sci. *126*, 3333-3343.
Soderholm, J.F., Bird, S.L., Kalab, P., Sampathkumar, Y., Hasegawa, K., Uehara-Bingen, M., Weis, K., and Heald, R. (2011). Importazole, a small molecule inhibitor of the transport receptor importin-β. ACS Chem Biol *6*, 700-708.
Stewart, M. (2007). Molecular mechanism of the nuclear protein import cycle. Nat Rev Mol Cell Biol *8*, 195-208.
Strom, A.C., and Weis, K. (2001). Importin-β-like nuclear transport receptors. Genome Biol *2*, REVIEWS3008.
Subramanian, K.S., Dziedzic, R.C., Nelson, H.N., Stern, M.E., Roggero, V.R., Bondzi, C., and Allison, L.A. (2015). Multiple exportins influence thyroid hormone receptor localization. Mol Cell Endocrinol. *411*, 86-96.
Tao, T., Lan, J., Lukacs, G.L., Hache, R.J., and Kaplan, F. (2006). Importin 13 regulates nuclear import of the glucocorticoid receptor in airway epithelial cells. Am J Respir Cell Mol Biol *35*, 668-680.
Tetenbaum-Novatt, J., and Rout, M.P. (2010). The mechanism of nucleocytoplasmic transport through the nuclear pore complex. Cold Spring Harb Symp Quant Biol *75*, 567-584.
Tran, E.J., King, M.C., and Corbett, A.H. (2014). Macromolecular transport between the nucleus and the cytoplasm: Advances in mechanism and emerging links to disease. Biochim Biophys Acta *1843*, 2784-2795.
Twyffels, L., Gueydan, C., and Kruys, V. (2014). Transportin-1 and transportin-2: protein nuclear import and beyond. FEBS Lett *588*, 1857-1868.
Tzagarakis-Foster, C., and Privalsky, M.L. (1998). Phosphorylation of thyroid hormone receptors by protein kinase A regulates DNA recognition by specific inhibition of receptor monomer binding. J Biol Chem *273*, 10926-10932.
Umemoto, T., and Fujiki, Y. (2012). Ligand-dependent nucleo-cytoplasmic shuttling of peroxisome proliferator-activated receptors, PPARα and PPARγ. Genes Cells *17*, 576-596.
Vazquez-Iglesias, L., Lostale-Seijo, I., Martinez-Costas, J., and Benavente, J. (2009). Avian reovirus sigmaA localizes to the nucleolus and enters the nucleus by a nonclassical energy- and carrier-independent pathway. J Virol *83*, 10163-10175.
Vazquez-Iglesias, L., Lostale-Seijo, I., Martinez-Costas, J., and Benavente, J. (2012). Different intracellular distribution of avian reovirus core protein sigmaA in cells of avian and mammalian origin. Virology *432*, 495-504.

Waldmann, I., Walde, S., and Kehlenbach, R.H. (2007). Nuclear import of c-Jun is mediated by multiple transport receptors. J Biol Chem *282*, 27685-27692.
Walther, R.F., Lamprecht, C., Ridsdale, A., Groulx, I., Lee, S., Lefebvre, Y.A., and Hache, R.J. (2003). Nuclear export of the glucocorticoid receptor is accelerated by cell fusion-dependent release of calreticulin. J Biol Chem *278*, 37858-37864.
Weinmann, L., Hock, J., Ivacevic, T., Ohrt, T., Mutze, J., Schwille, P., Kremmer, E., Benes, V., Urlaub, H., and Meister, G. (2009). Importin 8 is a gene silencing factor that targets argonaute proteins to distinct mRNAs. Cell *136*, 496-507.
Wente, S.R., and Rout, M.P. (2010). The nuclear pore complex and nuclear transport. Cold Spring Harb Perspect Biol *2*, a000562.
Xu, D., Farmer, A., and Chook, Y.M. (2010). Recognition of nuclear targeting signals by karyopherin-β proteins. Curr Opin Struct Biol *20*, 782-790.
Zhu, X.-G., Hanover, J.A., Hager, G.L., and Cheng, S.-y. (1998). Hormone-induced translocation of thyroid hormone receptors in living cells visualized using a receptor green fluorescent protein chimera. J Biol Chem *273*, 27058-27063.

Figure Legends

Fig. 1. *In vitro* nuclear import of TRα1 requires soluble factors and is temperature and energy-dependent. (A) Digitonin-permeabilized HeLa cells were incubated with import reaction mix containing FITC-GST-TRα1 as substrate, under the conditions indicated: 30ºC or 4ºC followed by 30ºC, with an energy regeneration system or apyrase, and in the presence or absence of rabbit reticulocyte lysate (RRL) as a source of replacement cytosol. After 30 min, samples were fixed, mounted, and viewed by fluorescence microscopy. In the presence of RRL, TRα1 was localized to the nucleus. In the absence of RRL, and in chilled or energy-depleted cells, TRα1 did not accumulate in the nucleus. Scale bar = 10 μm. (B) Quantification of TRα1 nuclear localization. Bars indicate the mean percentage of cells with nuclear accumulation of TRα1 (n=4-5 independent, biologically separate replicate experiments, with 200 cells per replicate) and error bars indicate ± SEM. ***P<0.001; **P<0.01; *P<0.05.

Fig. 2. RNAi specifically knocks down selected importins. (A) HeLa cells were transfected with importin-specific shRNA plasmids or a scrambled shRNA plasmid as a control, as indicated. RT-qPCR was used to confirm knockdown of importin mRNA levels. Bars indicate the mean relative expression level of importin mRNA in cells treated with importin-specific shRNA versus control cells, normalized to the levels of the housekeeping mRNA GAPDH. Error bars indicate ± SEM (n=3 independent, biologically separate replicates). (B) Immunoblot analysis was used to confirm knockdown of importin protein levels, as indicated. Bars indicate the mean relative expression level of importin proteins in cells treated with importin-specific shRNA (knockdown) relative to cells treated with the scrambled shRNA control, normalized to levels of GAPDH. Error bars indicate ± SEM (n=3 independent, biologically separate replicates). (C) Knockdown is specific for the selected importin. Immunoblot analysis was used to confirm that knockdown of a target importin with a specific shRNA, as indicated, did not have an effect on expression levels of other importins.

Fig. 3. Knockdown of importin β1 (Imp β1) and importin 7 (Ipo 7) by RNAi reduces nuclear accumulation of TRα1. (A) HeLa cells cotransfected with shRNA and GFP-TRα1 expression plasmids, as indicated, were analyzed by fluorescence microscopy after staining with DAPI to visualize the nucleus. Scale bar = 10 μm. (B) HeLa cells cotransfected with shRNA and GFP-TRα1 expression plasmids were fixed and scored for TRα1 localization: N, completely nuclear; N+C, nuclear and cytoplasmic (with distinct nucleus); WC, whole cell (nucleus not distinct). Bars indicate the mean percentage of cells in a

given category (n=3 independent, biologically separate replicate experiments, with 100 cells per replicate), and error bars indicate ± SEM. ***P<0.001; **P<0.01.

Fig. 4. Knockdown of importin α1 (Imp α1) by RNAi reduces nuclear accumulation of TRα1. HeLa cells were transfected with importin-specific shRNA plasmids or a scrambled shRNA plasmid as a control, as indicated. RT-qPCR (A) and immunoblots (B) were used to confirm knockdown of importin mRNA and protein levels, respectively. Error bars indicate ± SEM (n=3 independent, biologically separate replicates). (C) HeLa cells cotransfected with shRNA and GFP-TRα1 expression plasmids, as indicated, were analyzed by fluorescence microscopy. Scale bar = 10 μm. (D) HeLa cells cotransfected with shRNA and GFP-TRα1 expression plasmids were scored for TRα1 localization: N, completely nuclear; N+C, nuclear and cytoplasmic (with distinct nucleus); WC, whole cell (nucleus not distinct). Bars indicate the mean percentage of cells in a given category (n=3 independent, biologically separate replicate experiments, with 100 cells per replicate), and error bars indicate ± SEM. *P<0.05.

Fig. 5. Importazole reduces nuclear localization of TRα1 and TRβ1. HeLa cells were transfected with GFP-TRα1 (A) or GFP-TRβ1 (B) expression plasmids and untreated, treated with vehicle, or treated for 5 h with 50 μM importazole, a small molecule inhibitor of importin β1. Cells were then fixed and scored for localization of TRα1 or TRβ1: N, completely nuclear; N+C, nuclear and cytoplasmic (with distinct nucleus); WC, whole cell (nucleus not distinct). Bars indicate the mean percentage of cells in a given category (n=3 independent, biologically separate replicate experiments, with 200 to 400 cells per replicate), and error bars indicate ± SEM. ***P<0.001.

Fig. 6. Knockdown of importins 4, 5, 8, 9, 11, and 13 has no effect on nuclear accumulation of TRα1. (A) HeLa cells were transfected with importin (Ipo)-specific shRNA plasmids or a scrambled shRNA plasmid as a control, as indicated, and immunoblot analysis was used to confirm knockdown of importin protein levels. Error bars indicate ± SEM (n=3 independent, biologically separate replicates). (B) HeLa cells cotransfected with shRNA and GFP-TRα1 expression plasmids, as indicated, were analyzed by fluorescence microscopy after staining with DAPI to visualize the nucleus. Scale bar = 10 μm. (C) HeLa cells cotransfected with shRNA and GFP-TRα1 expression plasmids, as indicated, were scored for TRα1 localization: N, completely nuclear; N+C, nuclear and cytoplasmic (with distinct nucleus); WC, whole cell (nucleus not distinct). Bars indicate the mean percentage of cells in a given category (n=3 independent, biologically separate replicate experiments, with 100 cells per replicate), and error bars indicate ± SEM. P>0.05.

Fig. 7. Knockdown of importins 4, β1, 7, and α1 does not significantly alter TRα1-mediated gene expression. HeLa cells were cotransfected with expression plasmids for GFP-TRα1, TRE (DR+4)-firefly luciferase reporter, *Renilla* luciferase internal control, and scrambled shRNA control or a set of four target-specific shRNAs, as indicated. Data are presented as fold stimulation in the presence of T_3, relative to luciferase activity (firefly/*Renilla*) in the absence of T_3. Error bars indicate ± SEM (n=4 replicates of 8 wells per treatment). P>0.05.

Fig. 8. Importin β1, importin α1, and importin 7 coimmunoprecipitate with TRα1. HeLa cells were transfected with expression plasmids encoding GFP (27 kDa), GFP-TRα1 (73 kDa), GST-GFP-NLS (54 kDa), GFP-TRβ1 (79 kDa), GFP-GST-GFP (G3) (80 kDa), G3-A/BD (containing NLS-2) (86 kDa), or G3-Hinge (containing NLS-1) (87 kDa), as indicated. Cell lysates were subjected to coimmunoprecipitation using immobilized anti-GFP-antibodies (GFP-Trap®_A). Representative immunoblots are shown (n=3-5 independent, biologically separate replicate experiments). Protein size was verified using Pre-Stained Kaleidoscope Protein Standards. (A) Trapped GFP-tagged proteins were

analyzed by immunoblotting with antibodies specific for GFP. The two lower molecular weight bands in the GFP-TRα1 lane represent specific degradation products. (B) Immunosupernatants (Unbound) and immunoprecipitates (Bound) from GFP, GFP-TRα1, and GST-GFP-NLS-expressing cell lysates were analyzed on separate immunoblots (using longer exposure times for the immunoprecipitates), with importin-specific antibodies to detect importin 4 (119 kDa), importin α1 (58 kDa), importin β1 (97 kDa), and importin 7 (119 kDa), as indicated. The identity of the ~55 kDa band on the importin α1 immunoblot trapped by GST-GFP-NLS is not known. (C) Immunosupernatants (Unbound) and immunoprecipitates (Bound) from GFP and GFP- TRβ1-expressing cell lysates were analyzed by immunoblotting, with importin-specific antibodies, as indicated. (D) Immunosupernatants (Unbound) and immunoprecipitates (Bound) from G3-A/BD and GFP-Hinge-expressing cell lysates were analyzed by immunoblotting, with importin-specific antibodies, as indicated.

Figure 1

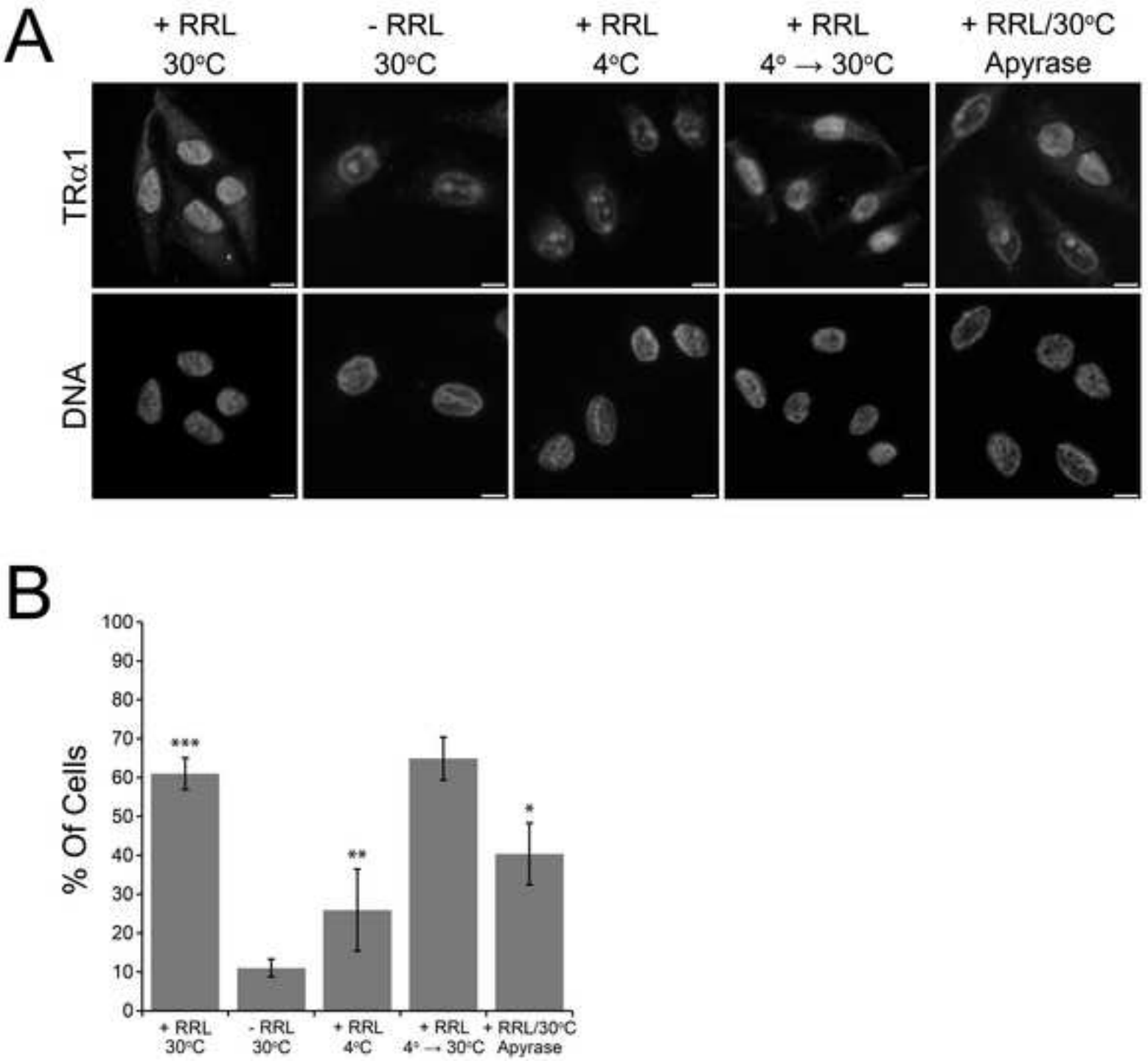
A
+ RRL 30°C
- RRL 30°C
+ RRL 4°C
+ RRL 4° → 30°C
+ RRL/30°C Apyrase
TRα1
DNA
B
% Of Cells
100
90
80
70
60
50
40
30
20
10
0
***
**
*
+ RRL 30°C
- RRL 30°C
+ RRL 4°C
+ RRL 4° → 30°C
+ RRL/30°C Apyrase

Figure 2

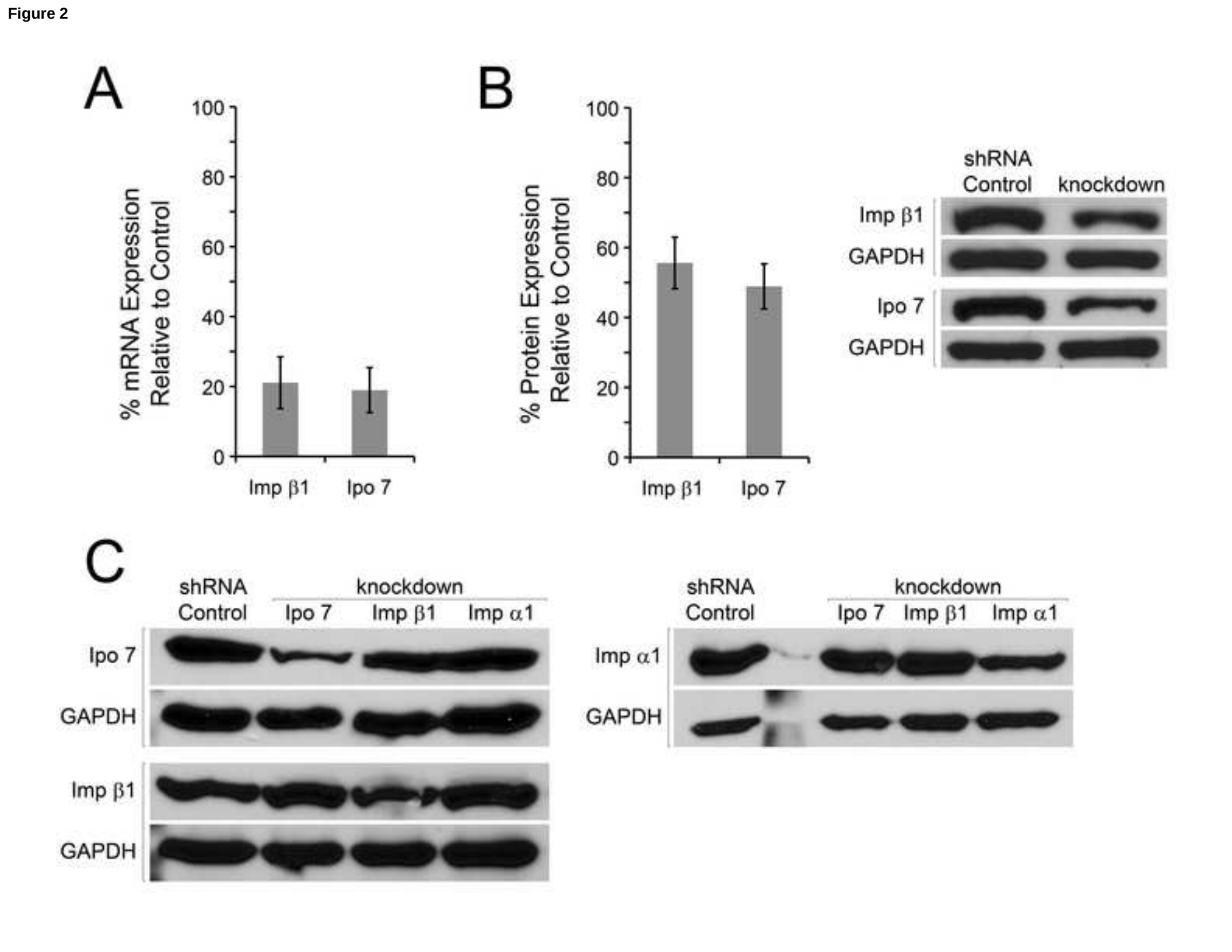
A
% mRNA Expression Relative to Control
100
80
60
40
20
0
Imp β1
Ipo 7
B
% Protein Expression Relative to Control
100
80
60
40
20
0
Imp β1
Ipo 7
shRNA Control
knockdown
Imp β1
GAPDH
Ipo 7
GAPDH
C
shRNA Control
knockdown
Ipo 7
Imp β1
Imp α1
Ipo 7
GAPDH
Imp β1
GAPDH
shRNA Control
knockdown
Ipo 7
Imp β1
Imp α1
Imp α1
GAPDH

Figure 3

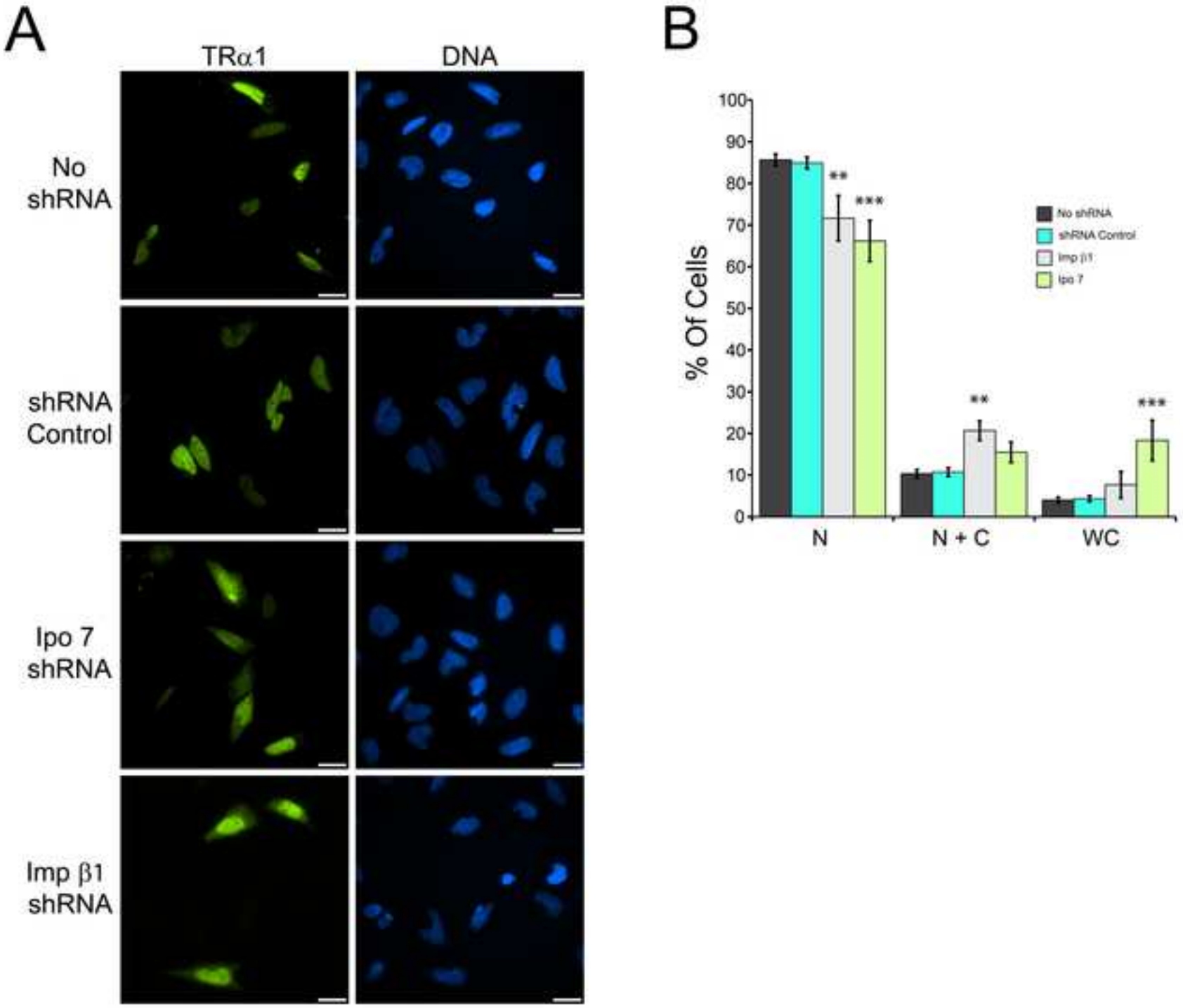
A
TRα1
DNA
No shRNA
shRNA Control
Ipo 7 shRNA
Imp β1 shRNA
B
% Of Cells
100
90
80
70
60
50
40
30
20
10
0
**
***
**
***
No shRNA
shRNA Control
Imp β1
Ipo 7
N
N + C
WC

Figure 4

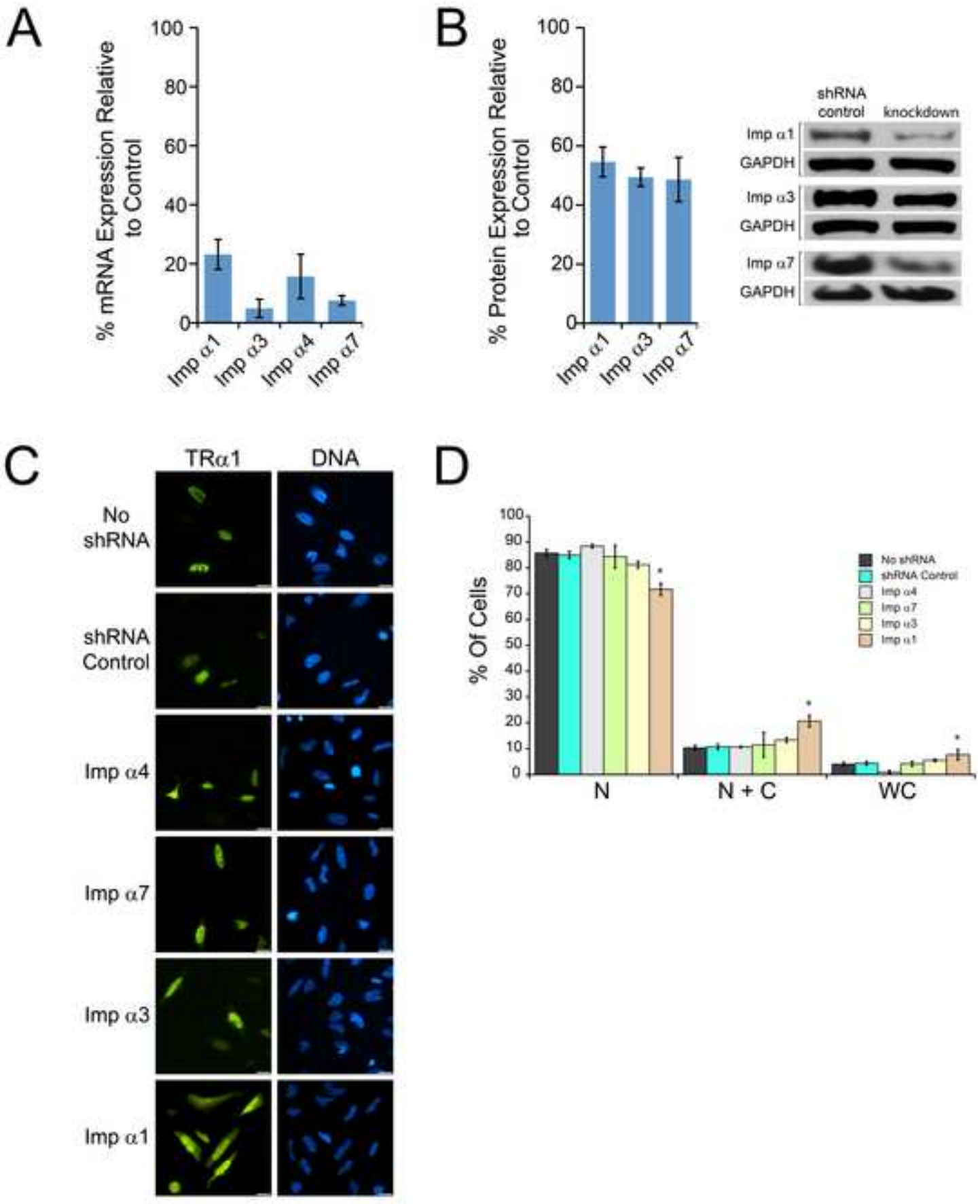
A
% mRNA Expression Relative to Control
100
80
60
40
20
0
Imp α1
Imp α3
Imp α4
Imp α7
B
% Protein Expression Relative to Control
100
80
60
40
20
0
Imp α1
Imp α3
Imp α7
shRNA control
knockdown
Imp α1
GAPDH
Imp α3
GAPDH
Imp α7
GAPDH
C
TRα1
DNA
No shRNA
shRNA Control
Imp α4
Imp α7
Imp α3
Imp α1
D
% Of Cells
100
90
80
70
60
50
40
30
20
10
0
N
N + C
WC
No shRNA
shRNA Control
Imp α4
Imp α7
Imp α3
Imp α1

Figure 5

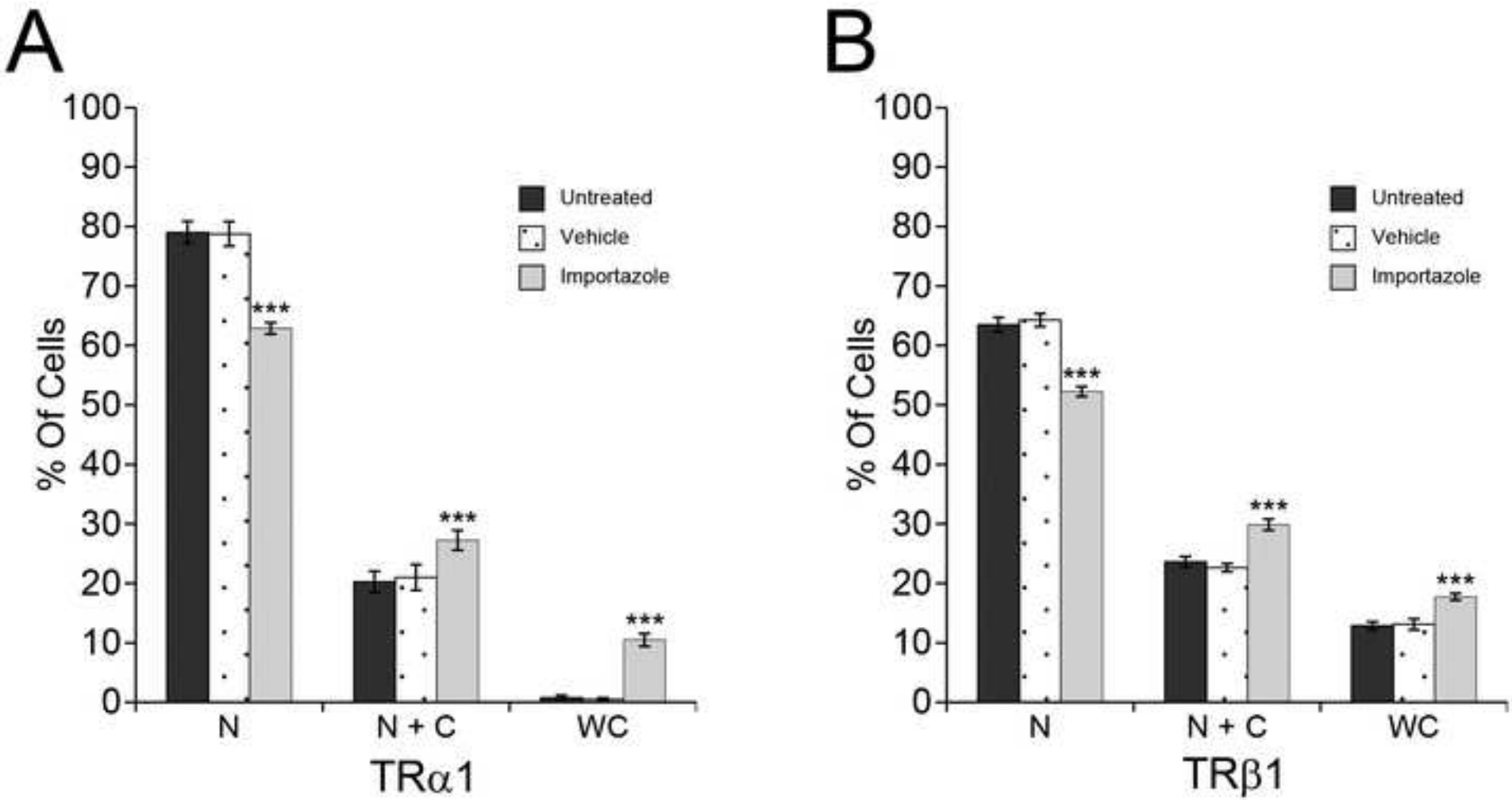
A
100
90
80
70
60
50
40
30
20
10
0
% Of Cells
Untreated
Vehicle
Importazole
***
***
***
N
N + C
WC
TRα1
B
100
90
80
70
60
50
40
30
20
10
0
% Of Cells
Untreated
Vehicle
Importazole
***
***
***
N
N + C
WC
TRβ1

Figure 6

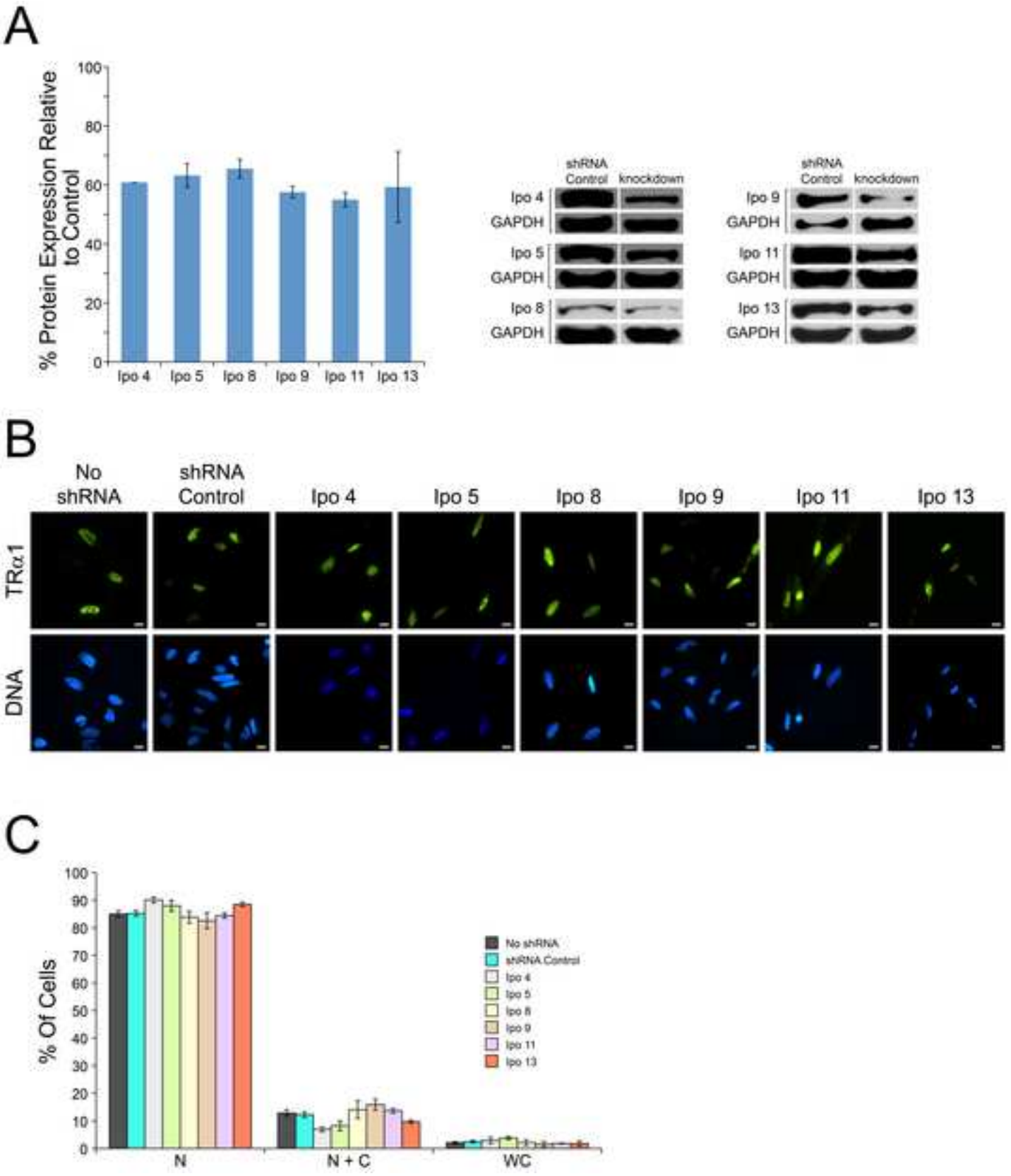
A
% Protein Expression Relative to Control
100
80
60
40
20
0
Ipo 4
Ipo 5
Ipo 8
Ipo 9
Ipo 11
Ipo 13
shRNA Control
knockdown
Ipo 4
GAPDH
Ipo 5
GAPDH
Ipo 8
GAPDH
Ipo 9
GAPDH
Ipo 11
GAPDH
Ipo 13
GAPDH
B
No shRNA
shRNA Control
Ipo 4
Ipo 5
Ipo 8
Ipo 9
Ipo 11
Ipo 13
TRα1
DNA
C
% Of Cells
100
90
80
70
60
50
40
30
20
10
0
N
N + C
WC
No shRNA
shRNA Control
Ipo 4
Ipo 5
Ipo 8
Ipo 9
Ipo 11
Ipo 13

Figure 7

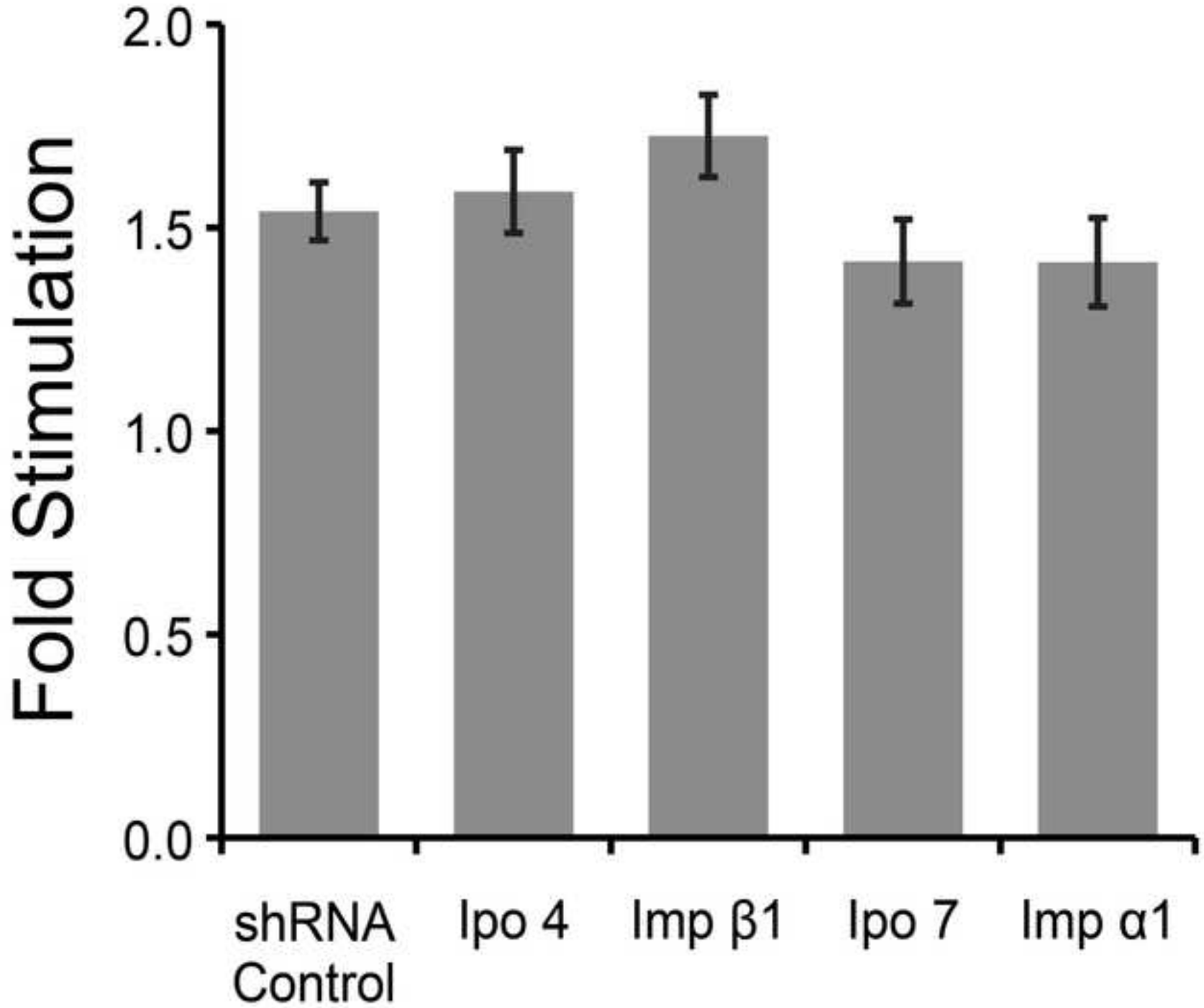
Fold Stimulation
2.0
1.5
1.0
0.5
0.0
shRNA Control
Ipo 4
Imp β1
Ipo 7
Imp α1

Figure 8

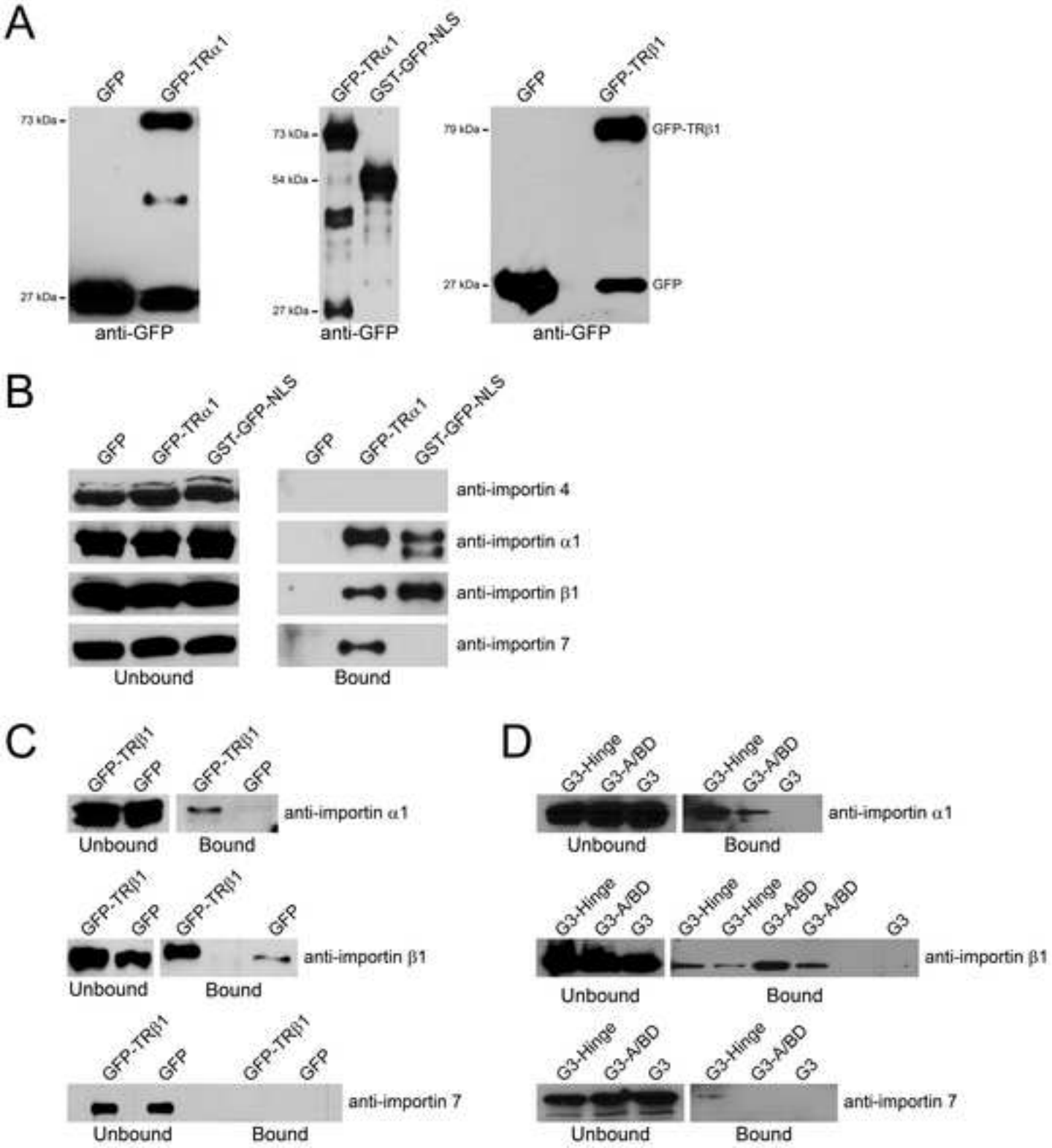
A
GFP
GFP-TRα1
73 kDa
27 kDa
anti-GFP
GFP-TRα1
GST-GFP-NLS
73 kDa
54 kDa
27 kDa
anti-GFP
GFP
GFP-TRβ1
79 kDa
GFP-TRβ1
27 kDa
GFP
anti-GFP
B
GFP
GFP-TRα1
GST-GFP-NLS
anti-importin 4
anti-importin α1
anti-importin β1
anti-importin 7
Unbound
Bound
C
GFP-TRβ1
GFP
anti-importin α1
Unbound
Bound
anti-importin β1
anti-importin 7
D
G3-Hinge
G3-A/BD
G3
anti-importin α1
anti-importin β1
anti-importin 7
Unbound
Bound